Effects of NO$_x$ and SO$_2$ on the Secondary Organic Aerosol Formation from Photooxidation of α-pinene and Limonene

Defeng Zhao[1], Sebastian H. Schmitt[1], Mingjin Wang[1, 2], Ismail-Hakki Acir[1, a], Ralf Tillmann[1], Zhaofeng Tan[1, 2], Anna Novelli[1], Hendrik Fuchs[1], Iida Pullinen[1, b], Robert Wegener[1], Franz Rohrer[1], Jürgen Wildt[1], Astrid Kiendler-Scharr[1], Andreas Wahner[1], Thomas F. Mentel[1]

[1] Institute of Energy and Climate Research, IEK-8: Troposphere, Forschungszentrum Jülich, Jülich, 52425, Germany

[2] College of Environmental Science and Engineering, Peking University, Beijing, 100871, China

[a]Now at: Institute of Nutrition and Food Sciences, University of Bonn, Bonn, 53115, Germany; [b]Now at: Department of Applied Physics, University of Eastern Finland, Kuopio, 7021, Finland.

Correspondence to: Th. F. Mentel (t.mentel@fz-juelich.de)

Abstract

Anthropogenic emissions such as NO$_x$ and SO$_2$ influence the biogenic secondary organic aerosol (SOA) formation, but detailed mechanisms and effects are still elusive. We studied the effects of NO$_x$ and SO$_2$ on the SOA formation from the photooxidation of α-pinene and limonene at ambient relevant NO$_x$ and SO$_2$ concentrations (NO$_x$: < 1 ppb to 20 ppb, SO$_2$: <0.05 ppb to 15 ppb). In these experiments, monoterpene oxidation was dominated by OH oxidation. We found that SO$_2$ induced nucleation and enhanced SOA mass formation. NO$_x$ strongly suppressed not only new particle formation but also SOA mass yield. However, in the presence of SO$_2$ which induced high number concentration of particles after oxidation to H$_2$SO$_4$, the suppression of the mass yield of SOA by NO$_x$ was completely or partly compensated. This indicates that the suppression of SOA yield by NO$_x$ was largely due to the suppressed new particle formation, leading to a lack of particle surface for the organics to condense on. By compensating for the suppressing effect on nucleation of NO$_x$, SO$_2$ also compensated for the suppressing effect on SOA yield. Aerosol mass spectrometer data show that increasing NO$_x$ enhanced nitrate formation. The majority of the nitrate was organic nitrate (57%-77%), even in low NO$_x$ conditions (<~1 ppb). Organic nitrate contributed 7%-26% of total organics assuming a molecular weight of 200 g/mol. SOA from α-pinene photooxidation at high NO$_x$ had generally lower hydrogen to carbon ratio (H/C), compared to low NO$_x$. The NO$_x$ dependence of the chemical composition can be attributed to the NO$_x$ dependence of the branching ratio of the RO$_2$ loss reactions, leading to lower fraction of organic hydroperoxides and higher fractions of organic nitrates at high NO$_x$. While NO$_x$ suppressed new particle formation and SOA mass formation, SO$_2$ can compensate for such effects, and the combining effect of SO$_2$ and NO$_x$ may have important influence on SOA formation affected by interactions of biogenic volatile organic compounds (VOC) with anthropogenic emissions.

1 Introduction

Secondary organic aerosol (SOA) have significant impacts on air quality, human health and climate change (Hallquist et al., 2009; Kanakidou et al., 2005; Jimenez et al., 2009; Zhang et al., 2011). SOA mainly originates

from biogenic volatile organic compounds (VOC) emitted by terrestrial vegetation (Hallquist et al., 2009). Once emitted into the atmosphere, biogenic VOC can undergo reactions with atmospheric oxidants including OH, O_3 and NO_3, and form SOA. When an air mass enriched in biogenic VOC is transported over an area with substantial anthropogenic emissions or vice versa, the reaction behavior of VOC and SOA formation can be altered due to the interactions of biogenic VOC with anthropogenic emissions such as NO_x, SO_2, anthropogenic aerosol and anthropogenic VOC. A number of field studies have highlighted the role of the anthropogenic-biogenic interactions in SOA formation (de Gouw et al., 2005; Goldstein et al., 2009; Hoyle et al., 2011; Worton et al., 2011; Glasius et al., 2011; Xu et al., 2015a; Shilling et al., 2012), which can induce an "anthropogenic enhancement" effect on SOA formation.

Among biogenic VOC, monoterpenes are important contributors to biogenic SOA due to their high emission rates, high reactivity and relative high SOA yield compared to isoprene (Guenther et al., 1995; Guenther et al., 2012; Chung and Seinfeld, 2002; Pandis et al., 1991; Griffin et al., 1999; Hoffmann et al., 1997; Zhao et al., 2015; Carlton et al., 2009). The anthropogenic modulation of the SOA formation from monoterpene can have important impacts on regional and global biogenic SOA budget (Spracklen et al., 2011). The influence of various anthropogenic pollutants on SOA formation of monoterpene have been investigated by a number of laboratory studies (Sarrafzadeh et al., 2016; Zhao et al., 2016; Flores et al., 2014; Emanuelsson et al., 2013; Eddingsaas et al., 2012a; Offenberg et al., 2009; Kleindienst et al., 2006; Presto et al., 2005; Ng et al., 2007; Zhang et al., 1992; Pandis et al., 1991; Draper et al., 2015; Han et al., 2016). In particular, NO_x and SO_2 have been shown to affect SOA formation from monoterpene.

NO_x changes the fate of RO_2 radical formed in VOC oxidation and therefore can change reaction product distribution and aerosol formation. At low NO_x, RO_2 mainly react with HO_2, forming organic hydroperoxides. At high NO_x, RO_2 mainly react with NO, forming organic nitrate (Hallquist et al., 2009; Ziemann and Atkinson, 2012; Finlayson-Pitts and Pitts Jr., 1999). Some studies found that the SOA yield from α-pinene is higher at lower NO_x concentration for ozonolysis (Presto et al., 2005) and photooxidation (Ng et al., 2007; Eddingsaas et al., 2012a; Han et al., 2016; Stirnweis et al., 2017). The decrease of SOA yield with increasing NO_x was proposed to be due to the formation of more volatile products like organic nitrate under high NO_x conditions (Presto et al., 2005). In contrast, a recent study found that the suppressing effect of NO_x is in large part attributed to the effect of NO_x on OH concentration for the SOA from β-pinene oxidation, and after eliminating the effect of NO_x on OH concentration, SOA yield only varies by 20-30% (Sarrafzadeh et al., 2016). Beside the effect of NO_x on SOA yield, NO_x has been found to suppress the new particle formation from VOC directly emitted by Mediterranean trees (mainly monoterpenes) (Wildt et al., 2014) and β-pinene (Sarrafzadeh et al., 2016), thereby reducing condensational sink present during high NO_x experiments.

Regarding the effect of SO_2, the SOA yield of α-pinene photooxidation was found to increase with SO_2 concentration at high NO_x concentrations (SO_2: 0-252 ppb, NO_x: 242-543 ppb, α-pinene: 178-255 ppb) (Kleindienst et al., 2006) and the increase is attributed to the formation of H_2SO_4 acidic aerosol. Acidity of seed aerosol was also found to enhance particle yield of α-pinene at high NO_x (Offenberg et al. (2009): NO_x 100-120 ppb, α-pinene 69-160 ppb; Han et al. (2016): initial NO ~70 ppb, α-pinene 14-18 ppb). In constrast, Eddingsaas et al. (2012a) found that particle yield increases with aerosol acidity only in "high NO" condition (NO_x 800 ppb, α-pinene: 20-52 ppb), but is independent of the presence of seed aerosol or aerosol acidity in both "high NO_2"

75 condition (NO$_x$ 800 ppb)" and low NO$_x$ (NO$_x$ lower than the detection limit of the NO$_x$ analyzer). Similarly, at

76 low NO$_x$ (initial NO <0.3 ppb, α-pinene ~20 ppb), Han et al. (2016) found that the acidity of seed has no

77 significant effect on SOA yield from α-pinene photooxidation. In addition, SO$_2$ was found to influence the gas

78 phase oxidation products from α-pinene and β-pinene photooxidation, which is possibly due to the change in

79 OH/HO$_2$ ratio caused by SO$_2$ oxidation or SO$_3$ directly reacting with organic molecules (Friedman et al., 2016).

80   While these studies have provided valuable insights into the effects of NO$_x$ and SO$_2$ on SOA formation, a

81 number of questions still remain elusive. For example, many studies used very high NO$_x$ and SO$_2$ concentrations

82 (up to several hundreds of ppb). High NO$_x$ can make the RO$_2$ radical fate dominated by one single pathway (i.e.,

83 RO$_2$+NO or RO$_2$+NO$_2$) to investigate SOA yields and composition under such conditions. Yet, the effects of NO$_x$

84 and SO$_2$ at concentration ranges for ambient anthropogenic-biogenic interactions (sub ppb to several tens of ppb

85 for NO$_2$ and SO$_2$) have seldom been directly addressed. Moreover, many previous studies on the SOA formation

86 from monoterpene oxidation focus on ozonolysis or do not distinguish OH oxidation and ozonolysis in

87 photooxidation, and only a few studies on OH oxidation have been conducted (Eddingsaas et al., 2012a; Zhao et

88 al., 2015; McVay et al., 2016; Sarrafzadeh et al., 2016; Henry et al., 2012; Ng et al., 2007). More importantly,

89 studies that investigated the combined effects of NO$_x$ and SO$_2$ are scarce, although they are often co-emitted from

90 anthropogenic sources. According to previous studies, NO$_x$ can have a suppressing effect on SOA formation

91 while SO$_2$ can have an enhancing effect. NO$_x$ and SO$_2$ might have counteracting or synergistic effects in SOA

92 formation in the ambient atmosphere.

93   In this study, we investigated the effects of NO$_x$, SO$_2$ and their combining effects on SOA formation from the

94 photooxidation of α-pinene and limonene. α-pinene and limonene are two important monoterpenes with high

95 emission rates among monoterpenes (Guenther et al., 2012). OH oxidation dominated over ozonolysis in the

96 monoterpene oxidation in this study as determined by measured OH and O$_3$ concentrations. The relative

97 contributions of RO$_2$ loss reactions at low NO$_x$ and high NO$_x$ were quantified using measured HO$_2$, RO$_2$, and NO

98 concentrations. The effects on new particle formation, SOA yield and aerosol chemical composition were

99 examined. We used ambient relevant NO$_x$ and SO$_2$ concentrations so that the results can shed lights on the

100 mechanisms of interactions of biogenic VOC with anthropogenic emissions in the real atmosphere.

101 **2 Experimental**

102 **2.1   Experimental setup and instrumentation**

103   The experiments were performed in the SAPHIR chamber (Simulation of Atmospheric PHotochemistry In a

104 large Reaction chamber) at Forschungszentrum Jülich, Germany. The details of the chamber have been described

105 before (Rohrer et al., 2005; Zhao et al., 2015). Briefly, it is a 270 m^3 Teflon chamber using natural sunlight for

106 illumination. It is equipped with a louvre system to switch between light and dark conditions. The physical

107 parameters for chamber running such as temperature and relative humidity were recorded. The solar irradiation

108 was characterized and the photolysis frequency was derived (Bohn et al., 2005; Bohn and Zilken, 2005).

109   Gas and particle phase species were characterized using various instruments. OH, HO$_2$ and RO$_2$ concentrations

110 were measured using a laser induced fluorescence (LIF) system with details described by Fuchs et al. (2012). OH

111 was formed via HONO photolysis, which was produced from a photolytic process on the Teflon chamber wall

112 (Rohrer et al., 2005). From OH concentration, OH dose, the integral of OH concentration over time, was
113 calculated in order to better compare experiments with different OH levels. For example, experiments at high
114 NO_x in this study generally had higher OH concentrations due to the faster OH production by recycling of $HO_2\bullet$
115 and $RO_2\bullet$ to OH. The VOC were characterized using a Proton Transfer Reaction Time-of-Flight Mass
116 Spectrometer (PTR-ToF-MS) and Gas Chromatography-Mass spectrometer (GC-MS). NO_x, O_3 and SO_2
117 concentrations were characterized using a NO_x analyzer (ECO PHYSICS TR480), an O_3 analyzer (ANSYCO,
118 model O341M), and an SO_2 analyzer (Thermo Systems 43i), respectively. O_3 was formed in photochemical
119 reactions since NO_x, even in trace amount (<~1 ppbV), was present in this study. More details of these
120 instrumentation are described before (Zhao et al., 2015).

121   The number and size distribution of particles were measured using a condensation particle counter (CPC,
122 TSI, model 3786) and a scanning mobility particle sizer (SMPS, TSI, DMA 3081/CPC 3785). From particle
123 number measurement, the nucleation rate ($J_{2.5}$) was derived from the number concentration of particles larger than
124 2.5 nm as measured by CPC. Particle chemical composition was measured using a High-Resolution Time-of-
125 Flight Aerosol Mass Spectrometer (HR-ToF-AMS, Aerodyne Research Inc.). From the AMS data, oxygen to
126 carbon ratio (O/C), hydrogen to carbon ratio (H/C), and nitrogen to carbon ratio (N/C) were derived using a
127 method derived in the literature (Aiken et al., 2007; Aiken et al., 2008). An update procedure to determine the
128 elemental composition is reported by Canagaratna et al. (2015), showing the O/C and H/C derived from the
129 method of Aiken et al. (2008) may be underestimated. The H/C and O/C were also derived using the newer
130 approach by Canagaratna et al. (2015) and compared with the data derived from the Aiken et al. (2007) method.
131 The H/C values derived using the Canagaratna et al. (2015) method strongly correlated with the values derived
132 using Aiken et al. (2007) method (Fig. S1) and just increased by 27% as suggested by Canagaratna et al. (2015).
133 Similar results were found for O/C and there was just a difference of 11% in O/C. Since only relative difference
134 in elemental composition of SOA is studied here, only the data derived using Aiken et al. (2007) method are
135 shown as the conclusion was not affected by the methods chosen. The fractional contribution of organics in the
136 signals at m/z=44 and m/z=43 to total organics (f_{44} and f_{43}, respectively) were also derived.

137   SOA yields were calculated as the ratio of organic aerosol mass formed to the amount of VOC reacted.
138 The mass concentration of organic aerosol was derived using the total aerosol volume concentration measured by
139 SMPS multiplied by the volume fraction of organics with a density of 1 g cm^{-3} to better compare with previous
140 literature. In the experiments with added SO_2, sulfuric acid was formed upon photooxidation and partly
141 neutralized by background ammonia, which was introduced into the chamber mainly due to humidification. The
142 volume fraction of organics was derived based on volume additivity using the mass of organics and ammonium
143 sulfate/ammonium bisulfate from AMS and their respective density (1.32 g cm^{-3} for organic aerosol from one of
144 our previous studies (Flores et al., 2014) and the literature (Ng et al., 2007) and ~1.77 g cm^{-3} for ammonium
145 sulfate/ammonium bisulfate). According to the calculations based on the E-AIM model (Clegg et al., 1998;
146 Wexler and Clegg, 2002) (http://www.aim.env.uea.ac.uk/aim/ aim.php), there was no aqueous phase formed at
147 the relative humidity in the experiments of this study. The average RH for the period of monoterpene
148 photooxidation was 28-34% except for one experiment with average RH of 42% RH. The organic aerosol
149 concentration was corrected for the particle wall loss and dilution loss using the method described in Zhao et al.
150 (2015).

2.2 Experimental procedure

The SOA formation from α-pinene and limonene photooxidation was investigated at different NO_x and SO_2 levels. Four types of experiments were done: with neither NO_x nor SO_2 added (referred to as "low NO_x, low SO_2"), with only NO_x added (~ 20 ppb NO, referred to as "high NO_x, low SO_2"), with only SO_2 added (~15 ppb, referred to as "low NO_x, high SO_2"), and with both NO_x and SO_2 added (~20 ppb NO and ~15 ppb SO_2, referred to as "high NO_x, high SO_2"). For low NO_x conditions, background NO concentrations were around 0.05-0.2 ppb, and NO was mainly from the background photolytic process of Teflon chamber wall (Rohrer et al., 2005). For low SO_2 conditions, background SO_2 concentrations were below the detection limit of the SO_2 analyzer (0.05 ppb). In some experiments, a lower level of SO_2 (2 ppb, referred to as "moderate SO_2") was used to test the effect of SO_2 concentration. An overview of the experiments is shown in Table 1.

In a typical experiment, the chamber was humidified to ~75% RH first, and then VOC and NO, if applicable, were added to the chamber. Then the roof was opened to start photooxidation. In the experiments with SO_2, SO_2 was added and the roof was opened to initialize nucleation first and then VOC was added. The particle number concentration caused by SO_2 oxidation typically reached several 10^4 cm^{-3} (see Fig. 2 high SO_2 cases) and after VOC addition, no further nucleation occurred. Adding SO_2 first and initializing nucleation by SO_2 photooxidation ensured that enough nucleating particles were present when VOC oxidation started. SO_2 concentration decayed slowly in the experiments with SO_2 added and most of the SO_2 was still left (typically around 8 ppb from initial 15 ppb) at the end of an experiment due to its low reactivity with OH. Typical SO_2 time series in high SO_2 experiments are shown in Fig S2. The detailed conditions of the experiments are shown in Table S1. The experiments of α-pinene and limonene photooxidation were designed to keep the initial OH reactivity and thus OH loss rate constant so that the OH concentrations of these experiments were more comparable. Therefore, the concentration of limonene was around one-third of the concentration of α-pinene due to the higher OH reactivity of limonene.

2.3 Wall loss of organic vapors

The loss of organic vapors on chamber walls can influence SOA yield (Kroll et al., 2007; Zhang et al., 2014; Ehn et al., 2014; Sarrafzadeh et al., 2016; McVay et al., 2016; Nah et al., 2016; Matsunaga and Ziemann, 2010; Ye et al., 2016; Loza et al., 2010). The wall loss rate of organic vapors in our chamber was estimated by following the decay of organic vapor concentrations after photooxidation was stopped in the experiments with low particle surface area (~5×10^{-8} cm^2 cm^{-3}) and thus low condensational sink on particles. Such method is similar to the method used in previous studies (Ehn et al., 2014; Sarrafzadeh et al., 2016; Krechmer et al., 2016; Zhang et al., 2015). A high-resolution time-of-flight chemical ionization mass spectrometer (HR-ToF-CIMS, Aerodyne Research Inc.) with nitrate ion source ($^{15}NO_3^-$) was used to measure semi/low-volatile organic vapors. The details of the instrument were described in our previous studies (Ehn et al., 2014; Sarrafzadeh et al., 2016). The decay of vapors started from the time when the roof of the chamber was closed. The data were acquired at a time resolution of 4 s. A typical decay of low-volatile organics is shown in Fig. S3 and the first-order wall loss rate was determined to be around 6×10^{-4} s^{-1}.

The SOA yield was not directly corrected for the vapor wall loss, but the influence of vapor wall loss on SOA yield was estimated using the method in the study of Sarrafzadeh et al. (2016) and the details of the method

5

are described therein. Briefly, particle surface and chamber walls competed for the vapor loss (condensation) and the condensation on particles led to particle growth. The fraction of organic vapor loss to particles in the sum of the vapor loss to chamber walls and to particles (F_p) was calculated. The vapor loss to chamber walls was derived using the wall loss rate. The vapor loss to particles was derived using particle surface area concentration, molecular velocity and an accommodation coefficient α_p (Sarrafzadeh et al., 2016). $1/F_p$ (f_{corr}) provides the correction factor to obtain the "real" SOA yield. f_{corr} is a function of particle surface area concentration and accommodation coefficient as shown in Fig. S4. Here a range of 0.1-1 for α_p was used, which is generally in line with the ranges of α_p found by Nah et al. (2016) by fitting a vapor-particle dynamic model to experimental data. At a given α_p, the higher particle surface area, the lower f_{corr} and the lower the influence of vapor wall loss are because most vapors condense on particle surface and vice versa. At a given particle surface area, f_{corr} decreases with α_p because at higher α_p a larger fraction of vapors condenses on particles. An average molecular weight of 200 g/mol was used to estimate the influence of vapor wall loss. For the aerosol surface area range in most of the experiments in this study, the influence of vapor wall loss on SOA yield was relatively small (<~40% for particle surface area larger than 3×10^{-6} cm^2 cm^{-3}, Fig. S4). Yet, for the experiments at high NO_x and low SO_2 for α-pinene and limonene, the influence of vapor wall loss on SOA can be high due to the low particle surface area, especially at lower α_p.

3 Results and discussion

3.1 Chemical scheme: VOC oxidation pathway and RO_2 fate

In the photooxidation of VOC, OH and O_3 often co-exist and both contribute to VOC oxidation because O_3 formation in chamber studies is often unavoidable during photochemical reactions of VOC even in the presence of trace amount of NO_x. In order to study the mechanism of SOA formation, it is helpful to isolate one oxidation pathway from the other. In this study, the reaction rates of OH and ozone with VOC are quantified using measured OH and O_3 concentrations multiplied by rate constants (time series of VOC, OH, and O_3 are shown in Fig. S5). Typical OH and O_3 concentrations in an experiment were around $(1-15) \times 10^6$ molecules cm^{-3} and 0-50 ppb, respectively, depending on the VOC and NO_x concentrations added. For all the experiment in this study, the VOC loss was dominated by OH oxidation over ozonolysis (see Fig. S6 as an example). The relative importance of the reaction of OH and O_3 with monoterpenes was similar in the low NO_x and high NO_x experiments. At high NO_x, OH was often higher while more O_3 was also produced. The dominant role of OH oxidation in VOC loss makes the chemical scheme simple and it is easier to interpret than cases when both OH oxidation and ozonolysis are important.

As mentioned above, RO_2 fate, i.e., the branching of RO_2 loss among different pathways, has an important influence on the product distribution and thus on SOA composition, physicochemical properties, and yields. RO_2 can react with NO, HO_2, RO_2, or isomerize. The fate of RO_2 mainly depends on the concentrations of NO, HO_2 and RO_2. Here, the loss rates of RO_2 via different pathways were quantified using the measured HO_2, NO and RO_2 concentrations and the rate constants based on the MCM3.3 (Jenkin et al., 1997; Saunders et al., 2003) (*http://mcm.leeds.ac.uk/MCM.*). Measured HO_2 and RO_2 concentrations are shown in Fig. S7 as an example and the relative importance of different RO_2 reaction pathways is compared in Fig. 1, which is similar for both α-

226   pinene and limonene oxidation. In the low NO_x conditions of this study, RO_2+NO dominated the RO_2 loss rate in

227   the beginning of an experiment (Fig. 1a). The trace amount of NO (up to ~0.2 ppbV) was from the photolysis of

228   HONO, which was continuously produced from a photolytic process on chamber walls throughout an experiment

229   (Rohrer et al., 2005). But later in the experiment, RO_2+HO_2 contributed a significant fraction (up to ~40 %) to

230   RO_2 loss because of increasing HO_2 concentration and decreasing NO concentration. In the high NO_x conditions,

231   RO_2+NO overwhelmingly dominated the RO_2 loss rate (Fig. 1b), and with the decrease of NO in an experiment,

232   the total RO_2 loss rate decreased substantially (Fig. 1b). Since the main products of RO_2+HO_2 are organic

233   hydroperoxides, more organic hydroperoxides relative to organic nitrates are expected in the low NO_x conditions

234   here. The loss rate of RO_2+RO_2 was estimated to be ~10^{-4} s^{-1} using a reaction rate constant of 2.5×10^{-13}

235   molecules^{-1} cm^3 s^{-1} (Ziemann and Atkinson, 2012). This contribution is negligible compared to other pathways in

236   this study, although the reaction rate constants of RO_2+RO_2 are highly uncertain and may depend on specific RO_2

237   (Ziemann and Atkinson, 2012). Note that the RO_2 fate in the low and high NO_x conditions quantified here are

238   further used in the discussion below since the information of RO_2 fate is important for data interpretation of

239   experiments conducted at different NO_x levels (Wennberg, 2013).

3.2   Effects of NO_x and SO_2 on new particle formation

241   The effects of NO_x and SO_2 on new particle formation from α-pinene oxidation are shown in Fig. 2a. In

242   low SO_2 conditions, both the total particle number concentration and nucleation rate at high NO_x were lower than

243   those at low NO_x, indicating NO_x suppressed the new particle formation. The suppressing effect of NO_x on new

244   particle formation was in agreement with the findings of Wildt et al. (2014). This suppression is considered to be

245   caused by the increased fraction of RO_2+NO reaction, decreasing the importance of RO_2+RO_2 permutation

246   reactions. RO_2+RO_2 reaction products are believed to be involved in the new particle formation (Wildt et al.,

247   2014; Kirkby et al., 2016) and initial growth of particles by forming higher molecular weight products such as

248   highly oxidized multifunctional molecules (HOM) and their dimers and trimers (Ehn et al., 2014; Kirkby et al.,

249   2016).

250   In high SO_2 conditions, the nucleation rate and total number concentrations were high, regardless of NO_x

251   levels. The high concentration of particles was attributed to the new particle formation induced by H_2SO_4 alone

252   formed by SO_2 oxidation since the new particle formation occurred before VOC addition. The role of H_2SO_4 in

253   new particle formation has been well studied in previous studies (Berndt et al., 2005; Zhang et al., 2012; Sipila et

254   al., 2010; Kirkby et al., 2011; Almeida et al., 2013).

255   Similar suppression of new particle formation by NO_x and enhancement of new particle formation by

256   SO_2 photooxidation were found for limonene oxidation (Fig. 2b).

3.3   Effects of NO_x and SO_2 on SOA mass yield

3.3.1   Effect of NO_x

259   Figure 3a shows SOA yield at different NO_x for α-pinene oxidation. In order to make different

260   experiments more comparable, the SOA yield is plotted as a function of OH dose instead of reaction time. In low

261   SO_2 conditions, NO_x not only suppressed the new particle formation but also suppressed SOA mass yield.

262   Because NO_x suppressed new particle formation, the suppression of the SOA yield could be attributed to the lack

of new particles as seed and thus the lack of condensational sink, or to the decrease of condensable organic materials. We further found that when new particle formation was already enhanced by added SO_2, the SOA yield at high NO_x was comparable to that at low NO_x and the difference in SOA yield between high NO_x and low NO_x was much smaller (Fig. 3a). This finding can be attributed to two possible explanations. Firstly, NO_x did not significantly suppress the formation of low volatile condensable organic materials, although NO_x obviously suppressed the formation of products for nucleation. Secondly, NO_x did suppress the formation of low-volatility condensable organic materials via forming potentially more volatile compounds and in addition to that, the suppressed formation of condensable organic materials was compensated by the presence of SO_2, resulting in comparable SOA yield. Organic nitrates are a group of compounds formed at high NO_x, which have been proposed to be more volatile (Presto et al., 2005; Kroll et al., 2006). However, many organic nitrates formed by photooxidation in this study were highly oxidized organic molecules (HOMs) containing multi-functional groups besides nitrate group ($C_{7-10}H_{9-15}NO_{8-15}$). These compounds are expected to have low volatility and they are found to have an uptake coefficient on particles of ~1 (Pullinen et al., in preparation). Therefore, the suppressing effect of NO_x on SOA yield was mostly likely due to suppressed nucleation, i.e., the lack of particle surface as condensational sink.

For limonene oxidation, similar results of NO_x suppressing the particle mass formation have been found in low SO_2 conditions (Fig. 3b). Yet, in high SO_2 conditions, the SOA yield from limonene oxidation at high NO_x was still significantly lower than that at low NO_x, which is different from the findings for α-pinene SOA. The cause of this difference is currently unknown. Our data of SOA yield suggest that the products formed from limonene oxidation at high NO_x seemed to have higher average volatility than that at low NO_x.

The suppression of SOA mass formation by NO_x under low SO_2 conditions agrees with previous studies (Eddingsaas et al., 2012a; Wildt et al., 2014; Sarrafzadeh et al., 2016; Hatakeyama et al., 1991). For example, it was found that high concentration of NO_x (tens of ppb) suppressed mass yield of SOA formed from photooxidation of β-pinene, α-pinene and VOC emitted by Mediterranean trees (Wildt et al., 2014; Sarrafzadeh et al., 2016). And on the basis of the results by Eddingsaas et al. (2012a) , the SOA yield at high NO_x (referred to as "high NO" by the authors) is lower than at low NO_x in the absence of seed aerosol.

Our finding that the difference in SOA yield between high NO_x and low NO_x conditions was highly reduced at high SO_2 is also in line with the findings of some previous studies using seed aerosols (Sarrafzadeh et al., 2016; Eddingsaas et al., 2012a). For example, Sarrafzadeh et al. (2016) found that in the presence of seed aerosol, the suppressing effect of NO_x on the SOA yield from β-pinene photooxidation is substantially diminished and SOA yield only decreases by 20-30% in the NO_x range of <1 ppb to 86 ppb at constant OH concentrations. The data by Eddingsaas et al. (2012a) also showed that in presence of seed aerosol, the difference in the SOA yield between low NO_x and high NO_x is much decreased. However, our finding is in contrast with the findings in other studies (Presto et al., 2005; Ng et al., 2007; Han et al., 2016; Stirnweis et al., 2017), who reported much lower SOA yield at high NO_x than at low NO_x in presence of seed. The different findings in these studies from ours may be attributed to the difference in the reaction conditions such as VOC oxidation pathways (OH oxidation vs. ozonolysis), VOC and NO_x concentration ranges, NO/NO_2, OH concentrations as well as organic aerosol loading, which all affect SOA yield. The reaction conditions of this study often differ from those described in the literature (see Table S2).

302   The difference in these conditions can result in both different apparent dependence on specific

303   parameters and the varied SOA yield. For example, SOA yield from α-pinene photooxidation at low NO_x in this

304   study appeared to be much lower than that in Eddingsaas et al. (2012a). The difference between the SOA yield in

305   this study and some of previous studies and between the values in the literature can be attributed to several

306   reasons: 1) RO_2 fates may be different. For example, in our study at low NO_x, RO_2+NO account for a large

307   fraction of RO_2 loss while in Eddingsaas et al. (2012a) RO_2+HO_2 is the dominant pathway of RO_2 loss. This

308   difference in RO_2 fates may affect oxidation products distribution. 2) The organic aerosol loading of this study is

309   much lower than that some of previous studies (e.g., Eddingsaas et al. (2012a)) (see Fig. S9). SOA yields in this

310   study were also plotted versus organic aerosol loading to better compare with previous studies (Fig. S8 and S9).

311   3) The total particle surface area in this study may also differ from previous studies, which may influence the

312   apparent SOA yield due to vapor wall loss (the total particle surface area is often not reported in many previous

313   studies to compare with). 4) RH of this study is different from many previous studies, which often used very low

314   RH (<10%). It is important to emphasize that reaction conditions including the NO_x as well as SO_2 concentration

315   range and RH in this study were chosen to be relevant to the anthropogenic-biogenic interactions in the ambient

316   atmosphere. In addition, difference in the organic aerosol density used in yield calculation should be taken into

317   account. In this study, SOA yield was derived using a density of 1 g cm^{-3} to better compare with many previous

318   studies (e.g., (Henry et al., 2012)), while in some other studies SOA yield was derived using different density

319   (e.g., 1.32 g cm^{-3} in Eddingsaas et al. (2012a)).

320   **3.3.2   Effect of SO_2**

321   For both α-pinene and limonene, SO_2 was found to enhance the SOA mass yield at given NO_x levels,

322   especially for the high NO_x cases (Fig. 3). The enhancing effect of SO_2 on particle mass formation can be

323   attributed to two reasons. Firstly, SO_2 oxidation induced new particle formation, which provided more surface

324   and volume for further condensation of organic vapors. This is consistent with the finding that the enhancement

325   of SOA yield by SO_2 was more significant at high NO_x when the enhancement in nucleation was also more

326   significant. Secondly, H_2SO_4 formed by photooxidation of SO_2 can enhance SOA formation via acid-catalyzed

327   heterogeneous uptake, an important SOA formation pathway initially found from isoprene photooxidation (Jang

328   et al., 2002; Lin et al., 2012; Surratt et al., 2007) and later also in the photooxidation of other compound such as

329   anthropogenic VOC (Chu et al., 2016; Liu et al., 2016). For the products from monoterpene oxidation, such an

330   acid-catalyzed effect may also occur (Northcross and Jang, 2007; Wang et al., 2012; Lal et al., 2012; Zhang et al.,

331   2006; Ding et al., 2011; Iinuma et al., 2009) and in this study, the particles were acidic with the molar ratio of

332   NH_4^+ to SO_4^{2-} around 1.5-1.8, although no aqueous phase was formed.

333   We found that the SOA yield in the limonene oxidation at a moderate SO_2 level (2 ppb) was comparable

334   to the yield at high SO_2 (15 ppb) when similar particle number concentrations in both cases were formed. Both

335   yields were significantly higher than the yield at low SO_2 (<0.05 ppb, see Fig. S10). This comparison suggests

336   that the effect in enhancing new particle formation by SO_2 seems to be more important compared to the particle

337   acidity effect. The role of SO_2 in new particle formation is similar to adding seed aerosol and providing particle

338   surface for organics to condense. Artificially added seed aerosol has been shown to enhance SOA formation from

339   α-pinene and β-pinene oxidation (Ehn et al., 2014; Sarrafzadeh et al., 2016; Eddingsaas et al., 2012a). In some

340   other studies, it was found that the SOA yield from α-pinene oxidation is independent of initial seed surface area

341   (McVay et al., 2016; Nah et al., 2016). The difference in the literature may be due to the range of total surface

342   area of particles, reaction conditions and chamber setup. For example, the peak particle-to-chamber surface ratio

343   for α-pinene photooxidation in this study was 7.7×10^{-5} at high NO_x and low SO_2, much lower than the aerosol

344   surface area range in the studies by Nah et al. (2016) and McVay et al. (2016). A lower particle-to-chamber

345   surface ratio can lead to a larger fraction of organics lost on chamber walls. Hence, providing additional particle

346   surface by adding seed particles can increase the condensation of organics on particles and thus increase SOA

347   yield. However, once the surface area is high enough to inhibit condensation of vapors on chamber walls, further

348   enhancement of particle surface will not significantly enhance the yield (Sarrafzadeh et al., 2016).

349   Particle acidity may also play a role in affecting the SOA yield in the experiments with high SO_2. Particle

350   acidity was found to enhance the SOA yield from α-pinene photooxidation at high NO_x (Offenberg et al., 2009)

351   and "high NO" conditions (Eddingsaas et al., 2012a). Yet, in low NO_x condition, particle acidity was reported to

352   have no significant effect on the SOA yield from α-pinene photooxidation (Eddingsaas et al., 2012a; Han et al.,

353   2016). According to these findings, at low NO_x the enhancement of SOA yield in this study is attributed to the

354   effect of facilitating nucleation and providing more particle surface by SO_2 photooxidation. At high NO_x, the

355   effect in enhancing new particle formation by SO_2 photooxidation seems to be more important, although the

356   effect of particle acidity resulted from SO_2 photooxidation may also play a role.

357   SO_2 has been proposed to also affect gas phase chemistry of organics by changing the HO_2/OH or

358   forming SO_3 (Friedman et al., 2016). In this study, the effect of SO_2 on gas phase chemistry of organics was not

359   significant because of the much lower reactivity of SO_2 with OH compared with α-pinene and limonene

360   (Atkinson et al., 2004, 2006; Atkinson and Arey, 2003) and the low OH concentrations (2-3 orders of magnitude

361   lower than those in the study by Friedman et al. (2016)). Moreover, reactions of RO_2 with SO_2 was also not

362   important because the reaction rate constant is very low ($<10^{-14}$ molecule^{-1} cm^3 s^{-1}) (Lightfoot et al., 1992; Berndt

363   et al., 2015). In addition, from the AMS data of SOA formed at high SO_2 no significant organic fragments

364   containing sulfur were found. Also the fragment $CH_3SO_2^+$ from organic sulfate suggested by Farmer et al. (2010)

365   was not detected in our data. The absence of organic sulfate tracers is likely due to the lack of aqueous phase in

366   aerosol particles in this study. Therefore, the influence of SO_2 on gas phase chemistry of organics and further on

367   SOA yield via affecting gas phase chemistry is not important in this study.

368   The presence of high SO_2 enhanced the SOA mass yield at high NO_x conditions, which was even

369   comparable with the SOA yield at low NO_x for α-pinene oxidation. This finding indicates that the suppressing

370   effect of NO_x on SOA mass formation was compensated to large extent by the presence of SO_2. This has

371   important implications for SOA formation affected by anthropogenic-biogenic interactions in the real atmosphere

372   when SO_2 and NO_x often co-exist in relative high concentrations as discussed below.

373   **3.4   Effects of NO_x and SO_2 on SOA chemical composition**

374   The effects of NO_x and SO_2 on SOA chemical composition were analyzed on the basis of AMS data. We

375   found that NO_x enhanced nitrate formation. The ratio of the mass of nitrate to organics was higher at high NO_x

376   than at low NO_x regardless of the SO_2 level, and similar trends were found for SOA from α-pinene and limonene

377   oxidation (Fig. 4a). Higher nitrate to organics ratios were observed for SOA from limonene at high NO_x, which is

378   mainly due to the lower VOC/NO$_x$ ratio resulted from the lower concentrations of limonene (7 ppb) compared to

379   α-pinene (20 ppb) (see Table 1). Overall, the mass ratios of nitrate to organics ranged from 0.02 to 0.11

380   considering all the experiments in this study.

381   Nitrate formed can be either inorganic (such as HNO$_3$ from the reaction of NO$_2$ with OH) or organic (from

382   the reaction of RO$_2$ with NO). The ratio of NO$_2^+$ (*m/z*=46) to NO$^+$ (*m/z*=30) in the mass spectra detected by AMS

383   can be used to differentiate whether nitrate is organic or inorganic (Fry et al., 2009; Rollins et al., 2009; Farmer et

384   al., 2010; Kiendler-Scharr et al., 2016). Organic nitrate was considered to have a NO$_2^+$/NO$^+$ of ~0.1 and inorganic

385   NH$_4$NO$_3$ had a NO$_2^+$/NO$^+$ of ~0.31 with the instrument used in this study as determined from calibration

386   measurements. In this study, NO$_2^+$/NO$^+$ ratios ranged from 0.14 to 0.18, closer to the ratio of organic nitrate. The

387   organic nitrate was estimated to account for 57%-77% (molar fraction) of total nitrate considering both the low

388   NO$_x$ and high NO$_x$ conditions. This indicates that nitrate was mostly organic nitrate, even at low NO$_x$ in this

389   study.

390   In order to determine the contribution of organic nitrate to total organics, we estimated the molecular

391   weight of organic nitrates formed by α-pinene and limonene oxidation to be 200-300 g/mol, based on reaction

392   mechanisms ((Eddingsaas et al., 2012b) and MCM v3.3, via website: http://mcm.leeds.ac.uk/MCM.). We

393   assumed a molecular weight of 200 g/mol in order to make our results comparable to the field studies which used

394   similar molecular weight (Kiendler-Scharr et al., 2016). For this value, the organic nitrate compounds were

395   estimated to account for 7-26% of the total organics mass as measured by AMS in SOA. Organic nitrate fraction

396   in total organics was within the range of values found in a field observation in southeast US (5-12% in summer

397   and 9-25% in winter depending on the molecular weight of organic nitrate) using AMS (Xu et al., 2015b) and

398   particle organic nitrate content derived from the sum of speciated organic nitrates (around 1-17% considering

399   observed variability and 3% and 8% on average in the afternoon and at night, respectively) (Lee et al., 2016).

400   Note that the organic nitrate fraction observed in this study was lower than the mean value (42%) for a number of

401   European observation stations when organic nitrate is mainly formed by the reaction of VOC with NO$_3$

402   (Kiendler-Scharr et al., 2016).

403   Moreover, we found that the contribution of organic nitrate to total organics (calculated using a

404   molecular weight of 200 g/mol for organic nitrate) was higher at high NO$_x$ (Fig. 4b), although in some

405   experiments the ratios of NO$_2^+$ to NO$^+$ were too noisy to derive a reliable fraction of organic nitrate. This result is

406   consistent with the reaction scheme that at high NO$_x$, almost all RO$_2$ loss was switched to the reaction with NO,

407   which is expected to enhance the organic nitrate formation. Besides organic nitrate, the ratio of nitrogen to carbon

408   atoms (N/C) was also found to be higher at high NO$_x$ (Fig. S11). But after considering nitrate functional group

409   separately, N/C ratio was very low, generally <0.01, which indicates majority of the organic nitrogen existed in

410   the form of organic nitrate.

411   The chemical composition of organic components of SOA in terms of H/C and O/C ratios at different

412   NO$_x$ and SO$_2$ levels was further compared. For SOA from α-pinene photooxidation, in low SO$_2$ conditions, no

413   significant difference in H/C and O/C was found between SOA formed at low NO$_x$ and at high NO$_x$ within the

414   experimental uncertainties (Fig. 5). The variability of H/C and O/C at high NO$_x$ is large, mainly due to the low

415   particle mass and small particle size. In high SO$_2$ conditions, SOA formed at high NO$_x$ had the higher O/C and

416   lower H/C, which indicates that SOA components had higher oxidation state. The higher O/C at high NO$_x$ than at

417   low NO_x is partly due to the higher OH dose at high NO_x, although even at same OH dose O/C at high NO_x was

418   still slightly higher than at low NO_x in high SO_2 conditions.

419   For the SOA formed from limonene photooxidation, no significant difference in the H/C and O/C was

420   found between different NO_x and SO_2 conditions (Fig. S12), which is partly due to the low signal resulting from

421   low particle mass and small particle size in high NO_x conditions.

422   Due to the high uncertainties for some of the H/C and O/C data, the chemical composition was further

423   analyzed using f_{44} and f_{43} since f_{44} and f_{43} are less noisy (Fig. 6). For both α-pinene and limonene, SOA formed at

424   high NO_x generally had lower f_{43}. Because f_{43} generally correlates with H/C in organic aerosol (Ng et al., 2011),

425   lower f_{43} is indicative of lower H/C, which is consistent with the lower H/C at high NO_x observed for SOA from

426   α-pinene oxidation in high SO_2 conditions (Fig. 5). The lower f_{43} at high NO_x was evidenced in the oxidation of

427   α-pinene based on the data in a previous study (Chhabra et al., 2011). The lower H/C and f_{43} are likely to be

428   related to the reaction pathways. According to the reaction mechanism mentioned above, at low NO_x a significant

429   fraction of RO_2 reacted with HO_2 forming hydroperoxides, while at high NO_x almost all RO_2 reacted with NO

430   forming organic nitrates. Compared with organic nitrates, hydroperoxides have higher H/C ratio. The same

431   mechanism also caused higher organic nitrate fraction at high NO_x, as discussed above.

432   Detailed mass spectra of SOA were compared, shown in Fig 7. For α-pinene, in high SO_2 conditions,

433   mass spectra of SOA formed at high NO_x generally had higher intensity for CHOgt1 ("gt1" means greater than 1)

434   family ions, such as CO_2^+ (*m/z* 44), but lower intensity for CH family ions, such as $C_2H_3^+$ (*m/z* 15), $C_3H_3^+$ (*m/z* 39)

435   (Fig. 7b) than at low NO_x. In low SO_2 conditions, such difference is not apparent (Fig. 7a), partly due to the low

436   signal from AMS for SOA formed at high NO_x as discussed above. For both the high SO_2 and low SO_2 cases,

437   mass spectra of SOA at high NO_x show higher intensity of CHN1 family ions. This is also consistent with the

438   higher N/C ratio shown above. For SOA from limonene oxidation, SOA formed at high NO_x had lower mass

439   fraction at *m/z* 15 ($C_2H_3^+$), 28 (CO^+), 43 ($C_2H_3O^+$), 44 (CO_2^+), and higher mass fraction at *m/z* 27 (CHN^+, $C_2H_3^+$),

440   41 ($C_3H_5^+$), 55 ($C_4H_7^+$), 64 (C_4O^+) than at low NO_x (Fig. S13). It seems that overall mass spectra of the SOA from

441   limonene formed at high NO_x had higher intensity for CH family ions, but lower intensity for CHO1 family ions

442   than at low NO_x. Note that the differences in these *m/z* were based on the average spectra during the whole

443   reaction period and may not reflect the chemical composition at a certain time.

444   **4 Conclusion and implications**

445   We investigated the SOA formation from the photooxidation of α-pinene and limonene under different NO_x

446   and SO_2 conditions, when OH oxidation was the dominant oxidation pathway of monoterpenes. The fate of RO_2

447   was regulated by varying NO_x concentrations. We confirmed that NO_x suppressed new particle formation. NO_x

448   also suppressed SOA mass yield in the absence of SO_2. The suppression of SOA yield by NO_x was likely due to

449   the suppressed new particle formation, i.e., absence of sufficient particle surfaces for organic vapor to condense

450   on at high NO_x.

451   SO_2 enhanced SOA yield from α-pinene and limonene photooxidation. SO_2 oxidation produced high number

452   concentration of particles and compensated for the suppression of SOA yield by NO_x to a large extent. The

453   enhancement of SOA yield by SO_2 is likely to be mainly caused by facilitating nucleation by H_2SO_4, although the

454   contribution of acid-catalyzed heterogeneous uptake cannot be excluded.

NO_x promoted nitrate formation. The majority (57-77%) of nitrate was organic nitrate at both low NO_x and high NO_x, based on the estimate using the NO_2^+/NO^+ ratios from AMS data. The significant contribution of organic nitrate to nitrate may have important implications for deriving the hygroscopicity from chemical composition. For example, a number of studies derived the hygroscopicity parameter by linear combination of the hygroscopicity parameters of various components such as sulfate, nitrate, and organics, assuming all nitrates are inorganic nitrate (Wu et al., 2013; Cubison et al., 2008; Yeung et al., 2014; Bhattu and Tripathi, 2015; Jaatinen et al., 2014; Moore et al., 2012; Gysel et al., 2007). Because the hygroscopicity parameter of organic nitrate may be much lower than inorganic nitrate (Suda et al., 2014), such derivation may overestimate hygroscopicity.

Organic nitrate compounds are estimated to contribute 7-26% of the total organics using an average molecular weight of 200 g/mol for organic nitrate compounds and a higher contribution of organic nitrate was found at high NO_x. Generally, SOA formed at high NO_x has a lower H/C compared to that at low NO_x. The higher contribution of organic nitrate to total organics and lower H/C at high NO_x than at low NO_x is attributed to the reaction of RO_2 with NO, which produced more organic nitrates relative to organic hydroperoxides formed via the reaction of RO_2 with HO_2. The different chemical composition of SOA between high and low NO_x conditions may affect the physicochemical properties of SOA such as volatility, hygroscopicity, and optical properties and thus change the impact of SOA on environment and climate.

The different effects of NO_x and SO_2 on new particle formation and SOA mass yields have important implications for SOA formation affected by anthropogenic-biogenic interactions in the ambient atmosphere. When an air mass of anthropogenic origin is transported to an area enriched in biogenic VOC emissions or vice versa, anthropogenic-biogenic interactions occur. Such scenarios are common in the ambient atmosphere in many areas. For example, Kiendler-Scharr et al. (2016) shows that the organic nitrate concentrations are high in all the rural sites all over Europe, indicating the important influence of anthropogenic emissions in rural areas which are often enriched in biogenic emissions. [14]C analysis in several studies show that modern source carbon, from biogenic emission or biomass burning, account for large fractions of organic aerosol even in urban areas (Szidat et al., 2009; Weber et al., 2007; Sun et al., 2012), indicating the potential interactions of biogenic emissions with anthropogenic emissions in urban areas. In such cases, anthropogenic NO_x alone may suppress the new particle formation and SOA mass from biogenic VOC oxidation, as we found in this study. However, due to the co-existence of NO_x with SO_2, H_2SO_4 formed by SO_2 oxidation can counteract such suppression of particle mass because regardless of NO_x levels, H_2SO_4 can induce new particle formation especially in the presence of water, ammonia or amine (Berndt et al., 2005; Zhang et al., 2012; Sipila et al., 2010; Almeida et al., 2013; Kirkby et al., 2011; Chen et al., 2012). The overall effects on SOA mass depend on specific NO_x, SO_2 and VOC concentrations and VOC types as well as anthropogenic aerosol concentrations and can be a net suppressing, neutral, or enhancing effect. Such scheme is depicted in Fig. 8. Other anthropogenic emissions, such as primary anthropogenic aerosol and precursors of anthropogenic secondary aerosol, can have similar roles as SO_2. By affecting the concentrations of SO_2, NO_x, and anthropogenic aerosol, anthropogenic emissions may have important mediating impacts on biogenic SOA formation. Considering the effects of these factors in isolation may cause bias in predicting biogenic SOA concentrations. The combined impacts of SO_2, NO_x, and anthropogenic aerosol are also important to the estimate on how much organic aerosol concentrations will change with the ongoing and future reduction of anthropogenic emissions (Carlton et al., 2010).

References

Aiken, A. C., DeCarlo, P. F., and Jimenez, J. L.: Elemental analysis of organic species with electron ionization high-resolution mass spectrometry, Anal. Chem., 79, 8350-8358, 10.1021/ac071150w, 2007.

Aiken, A. C., Decarlo, P. F., Kroll, J. H., Worsnop, D. R., Huffman, J. A., Docherty, K. S., Ulbrich, I. M., Mohr, C., Kimmel, J. R., Sueper, D., Sun, Y., Zhang, Q., Trimborn, A., Northway, M., Ziemann, P. J., Canagaratna, M. R., Onasch, T. B., Alfarra, M. R., Prevot, A. S. H., Dommen, J., Duplissy, J., Metzger, A., Baltensperger, U., and Jimenez, J. L.: O/C and OM/OC ratios of primary, secondary, and ambient organic aerosols with high-resolution time-of-flight aerosol mass spectrometry, Environ. Sci. Technol., 42, 4478-4485, 10.1021/es703009q, 2008.

Almeida, J., Schobesberger, S., Kurten, A., Ortega, I. K., Kupiainen-Maatta, O., Praplan, A. P., Adamov, A., Amorim, A., Bianchi, F., Breitenlechner, M., David, A., Dommen, J., Donahue, N. M., Downard, A., Dunne, E., Duplissy, J., Ehrhart, S., Flagan, R. C., Franchin, A., Guida, R., Hakala, J., Hansel, A., Heinritzi, M., Henschel, H., Jokinen, T., Junninen, H., Kajos, M., Kangasluoma, J., Keskinen, H., Kupc, A., Kurten, T., Kvashin, A. N., Laaksonen, A., Lehtipalo, K., Leiminger, M., Leppa, J., Loukonen, V., Makhmutov, V., Mathot, S., McGrath, M. J., Nieminen, T., Olenius, T., Onnela, A., Petaja, T., Riccobono, F., Riipinen, I., Rissanen, M., Rondo, L., Ruuskanen, T., Santos, F. D., Sarnela, N., Schallhart, S., Schnitzhofer, R., Seinfeld, J. H., Simon, M., Sipila, M., Stozhkov, Y., Stratmann, F., Tome, A., Trostl, J., Tsagkogeorgas, G., Vaattovaara, P., Viisanen, Y., Virtanen, A., Vrtala, A., Wagner, P. E., Weingartner, E., Wex, H., Williamson, C., Wimmer, D., Ye, P. L., Yli-Juuti, T., Carslaw, K. S., Kulmala, M., Curtius, J., Baltensperger, U., Worsnop, D. R., Vehkamaki, H., and Kirkby, J.: Molecular understanding of sulphuric acid-amine particle nucleation in the atmosphere, Nature, 502, 359-+, 10.1038/nature12663, 2013.

Atkinson, R., and Arey, J.: Atmospheric degradation of volatile organic compounds, Chem. Rev., 103, 4605-4638, 10.1021/cr0206420, 2003.

Atkinson, R., Baulch, D. L., Cox, R. A., Crowley, J. N., Hampson, R. F., Hynes, R. G., Jenkin, M. E., Rossi, M. J., and Troe, J.: Evaluated kinetic and photochemical data for atmospheric chemistry: Volume I - gas phase reactions of O-x, HOx, NOx and SOx species, Atmos. Chem. Phys., 4, 1461-1738, 2004.

Atkinson, R., Baulch, D. L., Cox, R. A., Crowley, J. N., Hampson, R. F., Hynes, R. G., Jenkin, M. E., Rossi, M. J., and Troe, J.: Evaluated kinetic and photochemical data for atmospheric chemistry: Volume II - gas phase reactions of organic species, Atmos. Chem. Phys., 6, 3625-4055, 2006.

Berndt, T., Boge, O., Stratmann, F., Heintzenberg, J., and Kulmala, M.: Rapid formation of sulfuric acid particles at near-atmospheric conditions, Science, 307, 698-700, 10.1126/science.1104054, 2005.

Berndt, T., Richters, S., Kaethner, R., Voigtlander, J., Stratmann, F., Sipila, M., Kulmala, M., and Herrmann, H.: Gas-Phase Ozonolysis of Cycloalkenes: Formation of Highly Oxidized RO2 Radicals and Their Reactions with NO, NO2, SO2, and Other RO2 Radicals, J. Phys. Chem. A 119, 10336-10348, 10.1021/acs.jpca.5b07295, 2015.

Bhattu, D., and Tripathi, S. N.: CCN closure study: Effects of aerosol chemical composition and mixing state, J. Geophys. Res.-Atmos., 120, 766-783, 10.1002/2014jd021978, 2015.

Bohn, B., Rohrer, F., Brauers, T., and Wahner, A.: Actinometric measurements of NO2 photolysis frequencies in the atmosphere simulation chamber SAPHIR, Atmos. Chem. Phys., 5, 493-503, 2005.

Bohn, B., and Zilken, H.: Model-aided radiometric determination of photolysis frequencies in a sunlit atmosphere simulation chamber, Atmos. Chem. Phys., 5, 191-206, 2005.

Canagaratna, M. R., Jimenez, J. L., Kroll, J. H., Chen, Q., Kessler, S. H., Massoli, P., Hildebrandt Ruiz, L., Fortner, E., Williams, L. R., Wilson, K. R., Surratt, J. D., Donahue, N. M., Jayne, J. T., and Worsnop, D. R.: Elemental ratio measurements of organic compounds using aerosol mass spectrometry: characterization, improved calibration, and implications, Atmos. Chem. Phys., 15, 253-272, 10.5194/acp-15-253-2015, 2015.

Carlton, A. G., Wiedinmyer, C., and Kroll, J. H.: A review of Secondary Organic Aerosol (SOA) formation from isoprene, Atmos. Chem. Phys., 9, 4987-5005, 2009.

Carlton, A. G., Pinder, R. W., Bhave, P. V., and Pouliot, G. A.: To What Extent Can Biogenic SOA be Controlled?, Environ. Sci. Technol., 44, 3376-3380, 10.1021/es903506b, 2010.

Chen, M., Titcombe, M., Jiang, J. K., Jen, C., Kuang, C. A., Fischer, M. L., Eisele, F. L., Siepmann, J. I., Hanson, D. R., Zhao, J., and McMurry, P. H.: Acid-base chemical reaction model for nucleation rates

15

551 in the polluted atmospheric boundary layer, Proc. Nat. Acad. Sci. U.S.A., 109, 18713-18718,
552 10.1073/pnas.1210285109, 2012.
553 Chhabra, P. S., Ng, N. L., Canagaratna, M. R., Corrigan, A. L., Russell, L. M., Worsnop, D. R., Flagan,
554 R. C., and Seinfeld, J. H.: Elemental composition and oxidation of chamber organic aerosol, Atmos.
555 Chem. Phys., 11, 8827-8845, 10.5194/acp-11-8827-2011, 2011.
556 Chu, B. W., Zhang, X., Liu, Y. C., He, H., Sun, Y., Jiang, J. K., Li, J. H., and Hao, J. M.: Synergetic
557 formation of secondary inorganic and organic aerosol: effect of SO2 and NH3 on particle formation and
558 growth, Atmos. Chem. Phys., 16, 14219-14230, 10.5194/acp-16-14219-2016, 2016.
559 Chung, S. H., and Seinfeld, J. H.: Global distribution and climate forcing of carbonaceous aerosols, J.
560 Geophys. Res.-Atmos., 107, 4407, 10.1029/2001jd001397, 2002.
561 Clegg, S. L., Brimblecombe, P., and Wexler, A. S.: Thermodynamic model of the system H+-NH4+-
562 SO42--NO3--H2O at tropospheric temperatures, J. Phys. Chem. A 102, 2137-2154, 10.1021/jp973042r,
563 1998.
564 Cubison, M. J., Ervens, B., Feingold, G., Docherty, K. S., Ulbrich, I. M., Shields, L., Prather, K.,
565 Hering, S., and Jimenez, J. L.: The influence of chemical composition and mixing state of Los Angeles
566 urban aerosol on CCN number and cloud properties, Atmos. Chem. Phys., 8, 5649-5667, 10.5194/acp-
567 8-5649-2008, 2008.
568 de Gouw, J. A., Middlebrook, A. M., Warneke, C., Goldan, P. D., Kuster, W. C., Roberts, J. M.,
569 Fehsenfeld, F. C., Worsnop, D. R., Canagaratna, M. R., Pszenny, A. A. P., Keene, W. C., Marchewka,
570 M., Bertman, S. B., and Bates, T. S.: Budget of organic carbon in a polluted atmosphere: Results from
571 the New England Air Quality Study in 2002, J. Geophys. Res.-Atmos., 110, D16305,
572 10.1029/2004jd005623, 2005.
573 Ding, X. A., Wang, X. M., and Zheng, M.: The influence of temperature and aerosol acidity on biogenic
574 secondary organic aerosol tracers: Observations at a rural site in the central Pearl River Delta region,
575 South China, Atmos. Environ., 45, 1303-1311, 10.1016/j.atmosenv.2010.11.057, 2011.
576 Draper, D. C., Farmer, D. K., Desyaterik, Y., and Fry, J. L.: A qualitative comparison of secondary
577 organic aerosol yields and composition from ozonolysis of monoterpenes at varying concentrations of
578 NO2, Atmos. Chem. Phys., 15, 12267-12281, 10.5194/acp-15-12267-2015, 2015.
579 Eddingsaas, N. C., Loza, C. L., Yee, L. D., Chan, M., Schilling, K. A., Chhabra, P. S., Seinfeld, J. H.,
580 and Wennberg, P. O.: alpha-pinene photooxidation under controlled chemical conditions - Part 2: SOA
581 yield and composition in low- and high-NOx environments, Atmos. Chem. Phys., 12, 7413-7427,
582 10.5194/acp-12-7413-2012, 2012a.
583 Eddingsaas, N. C., Loza, C. L., Yee, L. D., Seinfeld, J. H., and Wennberg, P. O.: alpha-pinene
584 photooxidation under controlled chemical conditions - Part 1: Gas-phase composition in low- and high-
585 NOx environments, Atmos. Chem. Phys., 12, 6489-6504, 10.5194/acp-12-6489-2012, 2012b.
586 Ehn, M., Thornton, J. A., Kleist, E., Sipila, M., Junninen, H., Pullinen, I., Springer, M., Rubach, F.,
587 Tillmann, R., Lee, B., Lopez-Hilfiker, F., Andres, S., Acir, I. H., Rissanen, M., Jokinen, T.,
588 Schobesberger, S., Kangasluoma, J., Kontkanen, J., Nieminen, T., Kurten, T., Nielsen, L. B., Jorgensen,
589 S., Kjaergaard, H. G., Canagaratna, M., Dal Maso, M., Berndt, T., Petaja, T., Wahner, A., Kerminen, V.
590 M., Kulmala, M., Worsnop, D. R., Wildt, J., and Mentel, T. F.: A large source of low-volatility
591 secondary organic aerosol, Nature, 506, 476-479, 10.1038/nature13032, 2014.
592 Emanuelsson, E. U., Hallquist, M., Kristensen, K., Glasius, M., Bohn, B., Fuchs, H., Kammer, B.,
593 Kiendler-Scharr, A., Nehr, S., Rubach, F., Tillmann, R., Wahner, A., Wu, H. C., and Mentel, T. F.:
594 Formation of anthropogenic secondary organic aerosol (SOA) and its influence on biogenic SOA
595 properties, Atmos. Chem. Phys., 13, 2837-2855, 10.5194/acp-13-2837-2013, 2013.
596 Farmer, D. K., Matsunaga, A., Docherty, K. S., Surratt, J. D., Seinfeld, J. H., Ziemann, P. J., and
597 Jimenez, J. L.: Response of an aerosol mass spectrometer to organonitrates and organosulfates and
598 implications for atmospheric chemistry, Proc. Nat. Acad. Sci. U.S.A., 107, 6670-6675,
599 10.1073/pnas.0912340107, 2010.
600 Finlayson-Pitts, B. J., and Pitts Jr., J. N.: Chemistry of the upper and lower atmosphere: theory,
601 experiments, and applications, Academic Press, San Diego, 969 pp., 1999.
602 Flores, J. M., Zhao, D. F., Segev, L., Schlag, P., Kiendler-Scharr, A., Fuchs, H., Watne, A. K.,
603 Bluvshtein, N., Mentel, T. F., Hallquist, M., and Rudich, Y.: Evolution of the complex refractive index

in the UV spectral region in ageing secondary organic aerosol, Atmos. Chem. Phys., 14, 5793-5806, 10.5194/acp-14-5793-2014, 2014.

Friedman, B., Brophy, P., Brune, W. H., and Farmer, D. K.: Anthropogenic Sulfur Perturbations on Biogenic Oxidation: SO2 Additions Impact Gas-Phase OH Oxidation Products of alpha- and beta-Pinene, Environ. Sci. Technol., 50, 1269-1279, 10.1021/acs.est.5b05010, 2016.

Fry, J. L., Kiendler-Scharr, A., Rollins, A. W., Wooldridge, P. J., Brown, S. S., Fuchs, H., Dube, W., Mensah, A., dal Maso, M., Tillmann, R., Dorn, H. P., Brauers, T., and Cohen, R. C.: Organic nitrate and secondary organic aerosol yield from NO3 oxidation of beta-pinene evaluated using a gas-phase kinetics/aerosol partitioning model, Atmos. Chem. Phys., 9, 1431-1449, 2009.

Fuchs, H., Dorn, H. P., Bachner, M., Bohn, B., Brauers, T., Gomm, S., Hofzumahaus, A., Holland, F., Nehr, S., Rohrer, F., Tillmann, R., and Wahner, A.: Comparison of OH concentration measurements by DOAS and LIF during SAPHIR chamber experiments at high OH reactivity and low NO concentration, Atmos. Meas. Tech., 5, 1611-1626, 10.5194/amt-5-1611-2012, 2012.

Glasius, M., la Cour, A., and Lohse, C.: Fossil and nonfossil carbon in fine particulate matter: A study of five European cities, Journal of Geophysical Research: Atmospheres, 116, D11302, 10.1029/2011jd015646, 2011.

Goldstein, A. H., Koven, C. D., Heald, C. L., and Fung, I. Y.: Biogenic carbon and anthropogenic pollutants combine to form a cooling haze over the southeastern United States, Proc. Nat. Acad. Sci. U.S.A., 106, 8835-8840, 10.1073/pnas.0904128106, 2009.

Griffin, R. J., Cocker, D. R., Flagan, R. C., and Seinfeld, J. H.: Organic aerosol formation from the oxidation of biogenic hydrocarbons, J. Geophys. Res.-Atmos., 104, 3555-3567, 10.1029/1998jd100049, 1999.

Guenther, A., Hewitt, C. N., Erickson, D., Fall, R., Geron, C., Graedel, T., Harley, P., Klinger, L., Lerdau, M., McKay, W. A., Pierce, T., Scholes, B., Steinbrecher, R., Tallamraju, R., Taylor, J., and Zimmerman, P.: A global-model of natural volatile organic-compound emissions, J. Geophys. Res.-Atmos., 100, 8873-8892, 10.1029/94jd02950, 1995.

Guenther, A. B., Jiang, X., Heald, C. L., Sakulyanontvittaya, T., Duhl, T., Emmons, L. K., and Wang, X.: The Model of Emissions of Gases and Aerosols from Nature version 2.1 (MEGAN2.1): an extended and updated framework for modeling biogenic emissions, Geosci. Model Dev., 5, 1471-1492, 10.5194/gmd-5-1471-2012, 2012.

Gysel, M., Crosier, J., Topping, D. O., Whitehead, J. D., Bower, K. N., Cubison, M. J., Williams, P. I., Flynn, M. J., McFiggans, G. B., and Coe, H.: Closure study between chemical composition and hygroscopic growth of aerosol particles during TORCH2, Atmos. Chem. Phys., 7, 6131-6144, 2007.

Hallquist, M., Wenger, J. C., Baltensperger, U., Rudich, Y., Simpson, D., Claeys, M., Dommen, J., Donahue, N. M., George, C., Goldstein, A. H., Hamilton, J. F., Herrmann, H., Hoffmann, T., Iinuma, Y., Jang, M., Jenkin, M. E., Jimenez, J. L., Kiendler-Scharr, A., Maenhaut, W., McFiggans, G., Mentel, T. F., Monod, A., Prevot, A. S. H., Seinfeld, J. H., Surratt, J. D., Szmigielski, R., and Wildt, J.: The formation, properties and impact of secondary organic aerosol: current and emerging issues, Atmos. Chem. Phys., 9, 5155-5236, 2009.

Han, Y. M., Stroud, C. A., Liggio, J., and Li, S. M.: The effect of particle acidity on secondary organic aerosol formation from alpha-pinene photooxidation under atmospherically relevant conditions, Atmos. Chem. Phys., 16, 13929-13944, 10.5194/acp-16-13929-2016, 2016.

Hatakeyama, S., Izumi, K., Fukuyama, T., Akimoto, H., and Washida, N.: Reactions of oh with alpha-pinene and beta-pinene in air - estimate of global co production from the atmospheric oxidation of terpenes, J. Geophys. Res.-Atmos., 96, 947-958, 10.1029/90jd02341, 1991.

Henry, K. M., Lohaus, T., and Donahue, N. M.: Organic Aerosol Yields from alpha-Pinene Oxidation: Bridging the Gap between First-Generation Yields and Aging Chemistry, Environ. Sci. Technol., 46, 12347-12354, 10.1021/es302060y, 2012.

Hoffmann, T., Odum, J. R., Bowman, F., Collins, D., Klockow, D., Flagan, R. C., and Seinfeld, J. H.: Formation of organic aerosols from the oxidation of biogenic hydrocarbons, J. Atmos. Chem., 26, 189-222, 10.1023/a:1005734301837, 1997.

Hoyle, C. R., Boy, M., Donahue, N. M., Fry, J. L., Glasius, M., Guenther, A., Hallar, A. G., Hartz, K. H., Petters, M. D., Petaja, T., Rosenoern, T., and Sullivan, A. P.: A review of the anthropogenic

657   influence on biogenic secondary organic aerosol, Atmos. Chem. Phys., 11, 321-343, DOI 10.5194/acp-
658   11-321-2011, 2011.
659   Iinuma, Y., Boege, O., Kahnt, A., and Herrmann, H.: Laboratory chamber studies on the formation of
660   organosulfates from reactive uptake of monoterpene oxides, Phys. Chem. Chem. Phys., 11, 7985-7997,
661   10.1039/b904025k, 2009.
662   Jaatinen, A., Romakkaniemi, S., Anttila, T., Hyvarinen, A. P., Hao, L. Q., Kortelainen, A., Miettinen,
663   P., Mikkonen, S., Smith, J. N., Virtanen, A., and Laaksonen, A.: The third Pallas Cloud Experiment:
664   Consistency between the aerosol hygroscopic growth and CCN activity, Boreal Environment Research,
665   19, 368-382, 2014.
666   Jang, M. S., Czoschke, N. M., Lee, S., and Kamens, R. M.: Heterogeneous atmospheric aerosol
667   production by acid-catalyzed particle-phase reactions, Science, 298, 814-817, 10.1126/science.1075798,
668   2002.
669   Jenkin, M. E., Saunders, S. M., and Pilling, M. J.: The tropospheric degradation of volatile organic
670   compounds: A protocol for mechanism development, Atmos. Environ., 31, 81-104, 10.1016/s1352-
671   2310(96)00105-7, 1997.
672   Jimenez, J. L., Canagaratna, M. R., Donahue, N. M., Prevot, A. S. H., Zhang, Q., Kroll, J. H., DeCarlo,
673   P. F., Allan, J. D., Coe, H., Ng, N. L., Aiken, A. C., Docherty, K. S., Ulbrich, I. M., Grieshop, A. P.,
674   Robinson, A. L., Duplissy, J., Smith, J. D., Wilson, K. R., Lanz, V. A., Hueglin, C., Sun, Y. L., Tian, J.,
675   Laaksonen, A., Raatikainen, T., Rautiainen, J., Vaattovaara, P., Ehn, M., Kulmala, M., Tomlinson, J.
676   M., Collins, D. R., Cubison, M. J., Dunlea, E. J., Huffman, J. A., Onasch, T. B., Alfarra, M. R.,
677   Williams, P. I., Bower, K., Kondo, Y., Schneider, J., Drewnick, F., Borrmann, S., Weimer, S.,
678   Demerjian, K., Salcedo, D., Cottrell, L., Griffin, R., Takami, A., Miyoshi, T., Hatakeyama, S.,
679   Shimono, A., Sun, J. Y., Zhang, Y. M., Dzepina, K., Kimmel, J. R., Sueper, D., Jayne, J. T., Herndon,
680   S. C., Trimborn, A. M., Williams, L. R., Wood, E. C., Middlebrook, A. M., Kolb, C. E., Baltensperger,
681   U., and Worsnop, D. R.: Evolution of Organic Aerosols in the Atmosphere, Science, 326, 1525-1529,
682   10.1126/science.1180353, 2009.
683   Kanakidou, M., Seinfeld, J. H., Pandis, S. N., Barnes, I., Dentener, F. J., Facchini, M. C., Van
684   Dingenen, R., Ervens, B., Nenes, A., Nielsen, C. J., Swietlicki, E., Putaud, J. P., Balkanski, Y., Fuzzi,
685   S., Horth, J., Moortgat, G. K., Winterhalter, R., Myhre, C. E. L., Tsigaridis, K., Vignati, E., Stephanou,
686   E. G., and Wilson, J.: Organic aerosol and global climate modelling: a review, Atmos. Chem. Phys., 5,
687   1053-1123, 2005.
688   Kiendler-Scharr, A., Mensah, A. A., Friese, E., Topping, D., Nemitz, E., Prevot, A. S. H., Äijälä, M.,
689   Allan, J., Canonaco, F., Canagaratna, M., Carbone, S., Crippa, M., Dall Osto, M., Day, D. A., De Carlo,
690   P., Di Marco, C. F., Elbern, H., Eriksson, A., Freney, E., Hao, L., Herrmann, H., Hildebrandt, L.,
691   Hillamo, R., Jimenez, J. L., Laaksonen, A., McFiggans, G., Mohr, C., O'Dowd, C., Otjes, R.,
692   Ovadnevaite, J., Pandis, S. N., Poulain, L., Schlag, P., Sellegri, K., Swietlicki, E., Tiitta, P., Vermeulen,
693   A., Wahner, A., Worsnop, D., and Wu, H. C.: Ubiquity of organic nitrates from nighttime chemistry in
694   the European submicron aerosol, Geophys. Res. Lett., 43, 7735-7744, 10.1002/2016GL069239, 2016.
695   Kirkby, J., Curtius, J., Almeida, J., Dunne, E., Duplissy, J., Ehrhart, S., Franchin, A., Gagne, S., Ickes,
696   L., Kurten, A., Kupc, A., Metzger, A., Riccobono, F., Rondo, L., Schobesberger, S., Tsagkogeorgas, G.,
697   Wimmer, D., Amorim, A., Bianchi, F., Breitenlechner, M., David, A., Dommen, J., Downard, A., Ehn,
698   M., Flagan, R. C., Haider, S., Hansel, A., Hauser, D., Jud, W., Junninen, H., Kreissl, F., Kvashin, A.,
699   Laaksonen, A., Lehtipalo, K., Lima, J., Lovejoy, E. R., Makhmutov, V., Mathot, S., Mikkila, J.,
700   Minginette, P., Mogo, S., Nieminen, T., Onnela, A., Pereira, P., Petaja, T., Schnitzhofer, R., Seinfeld, J.
701   H., Sipila, M., Stozhkov, Y., Stratmann, F., Tome, A., Vanhanen, J., Viisanen, Y., Vrtala, A., Wagner,
702   P. E., Walther, H., Weingartner, E., Wex, H., Winkler, P. M., Carslaw, K. S., Worsnop, D. R.,
703   Baltensperger, U., and Kulmala, M.: Role of sulphuric acid, ammonia and galactic cosmic rays in
704   atmospheric aerosol nucleation, Nature, 476, 429-U477, 10.1038/nature10343, 2011.
705   Kirkby, J., Duplissy, J., Sengupta, K., Frege, C., Gordon, H., Williamson, C., Heinritzi, M., Simon, M.,
706   Yan, C., Almeida, J., Tröstl, J., Nieminen, T., Ortega, I. K., Wagner, R., Adamov, A., Amorim, A.,
707   Bernhammer, A.-K., Bianchi, F., Breitenlechner, M., Brilke, S., Chen, X., Craven, J., Dias, A., Ehrhart,
708   S., Flagan, R. C., Franchin, A., Fuchs, C., Guida, R., Hakala, J., Hoyle, C. R., Jokinen, T., Junninen, H.,
709   Kangasluoma, J., Kim, J., Krapf, M., Kürten, A., Laaksonen, A., Lehtipalo, K., Makhmutov, V.,
710   Mathot, S., Molteni, U., Onnela, A., Peräkylä, O., Piel, F., Petäjä, T., Praplan, A. P., Pringle, K., Rap,

711 A., Richards, N. A. D., Riipinen, I., Rissanen, M. P., Rondo, L., Sarnela, N., Schobesberger, S., Scott,
712 C. E., Seinfeld, J. H., Sipilä, M., Steiner, G., Stozhkov, Y., Stratmann, F., Tomé, A., Virtanen, A.,
713 Vogel, A. L., Wagner, A. C., Wagner, P. E., Weingartner, E., Wimmer, D., Winkler, P. M., Ye, P.,
714 Zhang, X., Hansel, A., Dommen, J., Donahue, N. M., Worsnop, D. R., Baltensperger, U., Kulmala, M.,
715 Carslaw, K. S., and Curtius, J.: Ion-induced nucleation of pure biogenic particles, Nature, 533, 521-526,
716 10.1038/nature17953, 2016.
717 Kleindienst, T. E., Edney, E. O., Lewandowski, M., Offenberg, J. H., and Jaoui, M.: Secondary organic
718 carbon and aerosol yields from the irradiations of isoprene and alpha-pinene in the presence of NOx and
719 SO2, Environ. Sci. Technol., 40, 3807-3812, 10.1021/es052446r, 2006.
720 Krechmer, J. E., Pagonis, D., Ziemann, P. J., and Jimenez, J. L.: Quantification of Gas-Wall Partitioning
721 in Teflon Environmental Chambers Using Rapid Bursts of Low-Volatility Oxidized Species Generated
722 in Situ, Environ. Sci. Technol., 50, 5757-5765, 10.1021/acs.est.6b00606, 2016.
723 Kroll, J. H., Ng, N. L., Murphy, S. M., Flagan, R. C., and Seinfeld, J. H.: Secondary organic aerosol
724 formation from isoprene photooxidation, Environ. Sci. Technol., 40, 1869-1877, 10.1021/es0524301,
725 2006.
726 Kroll, J. H., Chan, A. W. H., Ng, N. L., Flagan, R. C., and Seinfeld, J. H.: Reactions of semivolatile
727 organics and their effects on secondary organic aerosol formation, Environ. Sci. Technol., 41, 3545-
728 3550, 10.1021/es062059x, 2007.
729 Lal, V., Khalizov, A. F., Lin, Y., Galvan, M. D., Connell, B. T., and Zhang, R. Y.: Heterogeneous
730 Reactions of Epoxides in Acidic Media, J. Phys. Chem. A 116, 6078-6090, 10.1021/jp2112704, 2012.
731 Lee, B. H., Mohr, C., Lopez-Hilfiker, F. D., Lutz, A., Hallquist, M., Lee, L., Romer, P., Cohen, R. C.,
732 Iyer, S., Kurten, T., Hu, W., Day, D. A., Campuzano-Jost, P., Jimenez, J. L., Xu, L., Ng, N. L., Guo, H.,
733 Weber, R. J., Wild, R. J., Brown, S. S., Koss, A., de Gouw, J., Olson, K., Goldstein, A. H., Seco, R.,
734 Kim, S., McAvey, K., Shepson, P. B., Starn, T., Baumann, K., Edgerton, E. S., Liu, J., Shilling, J. E.,
735 Miller, D. O., Brune, W., Schobesberger, S., D'Ambro, E. L., and Thornton, J. A.: Highly functionalized
736 organic nitrates in the southeast United States: Contribution to secondary organic aerosol and reactive
737 nitrogen budgets, Proc. Nat. Acad. Sci. U.S.A., 113, 1516-1521, 10.1073/pnas.1508108113, 2016.
738 Lightfoot, P. D., Cox, R. A., Crowley, J. N., Destriau, M., Hayman, G. D., Jenkin, M. E., Moortgat, G.
739 K., and Zabel, F.: Organic peroxy-radicals - kinetics, spectroscopy and tropospheric chemistry,
740 Atmospheric Environment Part a-General Topics, 26, 1805-1961, 10.1016/0960-1686(92)90423-i,
741 1992.
742 Lin, Y. H., Zhang, Z. F., Docherty, K. S., Zhang, H. F., Budisulistiorini, S. H., Rubitschun, C. L., Shaw,
743 S. L., Knipping, E. M., Edgerton, E. S., Kleindienst, T. E., Gold, A., and Surratt, J. D.: Isoprene
744 Epoxydiols as Precursors to Secondary Organic Aerosol Formation: Acid-Catalyzed Reactive Uptake
745 Studies with Authentic Compounds, Environ. Sci. Technol., 46, 250-258, 10.1021/es202554c, 2012.
746 Liu, T., Wang, X., Hu, Q., Deng, W., Zhang, Y., Ding, X., Fu, X., Bernard, F., Zhang, Z., Lu, S., He,
747 Q., Bi, X., Chen, J., Sun, Y., Yu, J., Peng, P., Sheng, G., and Fu, J.: Formation of secondary aerosols
748 from gasoline vehicle exhaust when mixing with SO2, Atmos. Chem. Phys., 16, 675-689, 10.5194/acp-
749 16-675-2016, 2016.
750 Loza, C. L., Chan, A. W. H., Galloway, M. M., Keutsch, F. N., Flagan, R. C., and Seinfeld, J. H.:
751 Characterization of Vapor Wall Loss in Laboratory Chambers, Environ. Sci. Technol., 44, 5074-5078,
752 10.1021/es100727v, 2010.
753 Matsunaga, A., and Ziemann, P. J.: Gas-Wall Partitioning of Organic Compounds in a Teflon Film
754 Chamber and Potential Effects on Reaction Product and Aerosol Yield Measurements, Aerosol Sci.
755 Technol., 44, 881-892, 10.1080/02786826.2010.501044, 2010.
756 McVay, R. C., Zhang, X., Aumont, B., Valorso, R., Camredon, M., La, Y. S., Wennberg, P. O., and
757 Seinfeld, J. H.: SOA formation from the photooxidation of alpha-pinene: systematic exploration of the
758 simulation of chamber data, Atmos. Chem. Phys., 16, 2785-2802, 10.5194/acp-16-2785-2016, 2016.
759 Moore, R. H., Cerully, K., Bahreini, R., Brock, C. A., Middlebrook, A. M., and Nenes, A.:
760 Hygroscopicity and composition of California CCN during summer 2010, J. Geophys. Res.-Atmos.,
761 117, D00v12, 10.1029/2011jd017352, 2012.
762 Nah, T., McVay, R. C., Zhang, X., Boyd, C. M., Seinfeld, J. H., and Ng, N. L.: Influence of seed
763 aerosol surface area and oxidation rate on vapor wall deposition and SOA mass yields: a case study with
764 alpha-pinene ozonolysis, Atmos. Chem. Phys., 16, 9361-9379, 10.5194/acp-16-9361-2016, 2016.

Ng, N. L., Chhabra, P. S., Chan, A. W. H., Surratt, J. D., Kroll, J. H., Kwan, A. J., McCabe, D. C., Wennberg, P. O., Sorooshian, A., Murphy, S. M., Dalleska, N. F., Flagan, R. C., and Seinfeld, J. H.: Effect of NO(x) level on secondary organic aerosol (SOA) formation from the photooxidation of terpenes, Atmos. Chem. Phys., 7, 5159-5174, 2007.

Ng, N. L., Canagaratna, M. R., Jimenez, J. L., Chhabra, P. S., Seinfeld, J. H., and Worsnop, D. R.: Changes in organic aerosol composition with aging inferred from aerosol mass spectra, Atmos. Chem. Phys., 11, 6465-6474, 10.5194/acp-11-6465-2011, 2011.

Northcross, A. L., and Jang, M.: Heterogeneous SOA yield from ozonolysis of monoterpenes in the presence of inorganic acid, Atmos. Environ., 41, 1483-1493, 10.1016/j.atmosenv.2006.10.009, 2007.

Offenberg, J. H., Lewandowski, M., Edney, E. O., Kleindienst, T. E., and Jaoui, M.: Influence of Aerosol Acidity on the Formation of Secondary Organic Aerosol from Biogenic Precursor Hydrocarbons, Environ. Sci. Technol., 43, 7742-7747, 10.1021/es901538e, 2009.

Pandis, S. N., Paulson, S. E., Seinfeld, J. H., and Flagan, R. C.: Aerosol formation in the photooxidation of isoprene and beta-pinene, Atmospheric Environment Part a-General Topics, 25, 997-1008, 10.1016/0960-1686(91)90141-s, 1991.

Presto, A. A., Hartz, K. E. H., and Donahue, N. M.: Secondary organic aerosol production from terpene ozonolysis. 2. Effect of NOx concentration, Environ. Sci. Technol., 39, 7046-7054, 10.1021/es050400s, 2005.

Rohrer, F., Bohn, B., Brauers, T., Bruning, D., Johnen, F. J., Wahner, A., and Kleffmann, J.: Characterisation of the photolytic HONO-source in the atmosphere simulation chamber SAPHIR, Atmos. Chem. Phys., 5, 2189-2201, 2005.

Rollins, A. W., Kiendler-Scharr, A., Fry, J. L., Brauers, T., Brown, S. S., Dorn, H. P., Dube, W. P., Fuchs, H., Mensah, A., Mentel, T. F., Rohrer, F., Tillmann, R., Wegener, R., Wooldridge, P. J., and Cohen, R. C.: Isoprene oxidation by nitrate radical: alkyl nitrate and secondary organic aerosol yields, Atmos. Chem. Phys., 9, 6685-6703, 2009.

Sarrafzadeh, M., Wildt, J., Pullinen, I., Springer, M., Kleist, E., Tillmann, R., Schmitt, S. H., Wu, C., Mentel, T. F., Zhao, D. F., Hastie, D. R., and Kiendler-Scharr, A.: Impact of NOx and OH on secondary organic aerosol formation from beta-pinene photooxidation, Atmos. Chem. Phys., 16, 11237-11248, 10.5194/acp-16-11237-2016, 2016.

Saunders, S. M., Jenkin, M. E., Derwent, R. G., and Pilling, M. J.: Protocol for the development of the Master Chemical Mechanism, MCM v3 (Part A): tropospheric degradation of non-aromatic volatile organic compounds, Atmos. Chem. Phys., 3, 161-180, 2003.

Shilling, J. E., Zaveri, R. A., Fast, J. D., Kleinman, L., Alexander, M. L., Canagaratna, M. R., Fortner, E., Hubbe, J. M., Jayne, J. T., Sedlacek, A., Setyan, A., Springston, S., Worsnop, D. R., and Zhang, Q.: Enhanced SOA formation from mixed anthropogenic and biogenic emissions during the CARES campaign, Atmos. Chem. Phys. Discuss., 12, 26297-26349, 10.5194/acpd-12-26297-2012, 2012.

Sipila, M., Berndt, T., Petaja, T., Brus, D., Vanhanen, J., Stratmann, F., Patokoski, J., Mauldin, R. L., Hyvarinen, A. P., Lihavainen, H., and Kulmala, M.: The Role of Sulfuric Acid in Atmospheric Nucleation, Science, 327, 1243-1246, 10.1126/science.1180315, 2010.

Spracklen, D. V., Jimenez, J. L., Carslaw, K. S., Worsnop, D. R., Evans, M. J., Mann, G. W., Zhang, Q., Canagaratna, M. R., Allan, J., Coe, H., McFiggans, G., Rap, A., and Forster, P.: Aerosol mass spectrometer constraint on the global secondary organic aerosol budget, Atmos. Chem. Phys., 11, 12109-12136, 10.5194/acp-11-12109-2011, 2011.

Stirnweis, L., Marcolli, C., Dommen, J., Barmet, P., Frege, C., Platt, S. M., Bruns, E. A., Krapf, M., Slowik, J. G., Wolf, R., Prevot, A. S. H., Baltensperger, U., and El-Haddad, I.: Assessing the influence of NOx concentrations and relative humidity on secondary organic aerosol yields from alpha-pinene photo-oxidation through smog chamber experiments and modelling calculations, Atmos. Chem. Phys., 17, 5035-5061, 10.5194/acp-17-5035-2017, 2017.

Suda, S. R., Petters, M. D., Yeh, G. K., Strollo, C., Matsunaga, A., Faulhaber, A., Ziemann, P. J., Prenni, A. J., Carrico, C. M., Sullivan, R. C., and Kreidenweis, S. M.: Influence of Functional Groups on Organic Aerosol Cloud Condensation Nucleus Activity, Environ. Sci. Technol., 48, 10182-10190, 10.1021/es502147y, 2014.

817 Sun, X. S., Hu, M., Guo, S., Liu, K. X., and Zhou, L. P.: C-14-Based source assessment of
818 carbonaceous aerosols at a rural site, Atmos. Environ., 50, 36-40, 10.1016/j.atmosenv.2012.01.008,
819 2012.
820 Surratt, J. D., Lewandowski, M., Offenberg, J. H., Jaoui, M., Kleindienst, T. E., Edney, E. O., and
821 Seinfeld, J. H.: Effect of acidity on secondary organic aerosol formation from isoprene, Environ. Sci.
822 Technol., 41, 5363-5369, 10.1021/es0704176, 2007.
823 Szidat, S., Ruff, M., Perron, N., Wacker, L., Synal, H. A., Hallquist, M., Shannigrahi, A. S., Yttri, K. E.,
824 Dye, C., and Simpson, D.: Fossil and non-fossil sources of organic carbon (OC) and elemental carbon
825 (EC) in Goteborg, Sweden, Atmos. Chem. Phys., 9, 1521-1535, 10.5194/acp-9-1805-2009, 2009.
826 Wang, T. H., Liu, Z., Wang, W. G., and Ge, M. F.: Heterogeneous Uptake Kinetics of Limonene and
827 Limonene Oxide by Sulfuric Acid Solutions, Acta Phys. Chim. Sin. , 28, 1608-1614,
828 10.3866/pku.whxb201204241, 2012.
829 Weber, R. J., Sullivan, A. P., Peltier, R. E., Russell, A., Yan, B., Zheng, M., de Gouw, J., Warneke, C.,
830 Brock, C., Holloway, J. S., Atlas, E. L., and Edgerton, E.: A study of secondary organic aerosol
831 formation in the anthropogenic-influenced southeastern United States, J. Geophys. Res.-Atmos., 112,
832 D13302, 10.1029/2007jd008408, 2007.
833 Wennberg, P. O.: Let's abandon the "high NOx" and "low NOx" terminology, IGAC News, 3−4, 2013.
834 Wexler, A. S., and Clegg, S. L.: Atmospheric aerosol models for systems including the ions H+, NH4+,
835 Na+, SO42-, NO3-,Cl-, Br-, and H2O, J. Geophys. Res.-Atmos., 107, 4207, 10.1029/2001jd000451,
836 2002.
837 Wildt, J., Mentel, T. F., Kiendler-Scharr, A., Hoffmann, T., Andres, S., Ehn, M., Kleist, E., Müsgen, P.,
838 Rohrer, F., Rudich, Y., Springer, M., Tillmann, R., and Wahner, A.: Suppression of new particle
839 formation from monoterpene oxidation by NOx, Atmos. Chem. Phys., 14, 2789-2804, 10.5194/acp-14-
840 2789-2014, 2014.
841 Worton, D. R., Goldstein, A. H., Farmer, D. K., Docherty, K. S., Jimenez, J. L., Gilman, J. B., Kuster,
842 W. C., de Gouw, J., Williams, B. J., Kreisberg, N. M., Hering, S. V., Bench, G., McKay, M.,
843 Kristensen, K., Glasius, M., Surratt, J. D., and Seinfeld, J. H.: Origins and composition of fine
844 atmospheric carbonaceous aerosol in the Sierra Nevada Mountains, California, Atmos. Chem. Phys., 11,
845 10219-10241, 10.5194/acp-11-10219-2011, 2011.
846 Wu, Z. J., Poulain, L., Henning, S., Dieckmann, K., Birmili, W., Merkel, M., van Pinxteren, D.,
847 Spindler, G., Muller, K., Stratmann, F., Herrmann, H., and Wiedensohler, A.: Relating particle
848 hygroscopicity and CCN activity to chemical composition during the HCCT-2010 field campaign,
849 Atmos. Chem. Phys., 13, 7983-7996, 10.5194/acp-13-7983-2013, 2013.
850 Xu, L., Guo, H. Y., Boyd, C. M., Klein, M., Bougiatioti, A., Cerully, K. M., Hite, J. R., Isaacman-
851 VanWertz, G., Kreisberg, N. M., Knote, C., Olson, K., Koss, A., Goldstein, A. H., Hering, S. V., de
852 Gouw, J., Baumann, K., Lee, S. H., Nenes, A., Weber, R. J., and Ng, N. L.: Effects of anthropogenic
853 emissions on aerosol formation from isoprene and monoterpenes in the southeastern United States,
854 Proc. Nat. Acad. Sci. U.S.A., 112, 37-42, 10.1073/pnas.1417609112, 2015a.
855 Xu, L., Suresh, S., Guo, H., Weber, R. J., and Ng, N. L.: Aerosol characterization over the southeastern
856 United States using high-resolution aerosol mass spectrometry: spatial and seasonal variation of aerosol
857 composition and sources with a focus on organic nitrates, Atmos. Chem. Phys., 15, 7307-7336,
858 10.5194/acp-15-7307-2015, 2015b.
859 Ye, P. L., Ding, X., Hakala, J., Hofbauer, V., Robinson, E. S., and Donahue, N. M.: Vapor wall loss of
860 semi-volatile organic compounds in a Teflon chamber, Aerosol Sci. Technol., 50, 822-834,
861 10.1080/02786826.2016.1195905, 2016.
862 Yeung, M. C., Lee, B. P., Li, Y. J., and Chan, C. K.: Simultaneous HTDMA and HR-ToF-AMS
863 measurements at the HKUST Supersite in Hong Kong in 2011, J. Geophys. Res.-Atmos., 119, 9864-
864 9883, 10.1002/2013jd021146, 2014.
865 Zhang, J. Y., Hartz, K. E. H., Pandis, S. N., and Donahue, N. M.: Secondary organic aerosol formation
866 from limonene ozonolysis: Homogeneous and heterogeneous influences as a function of NOx, J. Phys.
867 Chem. A 110, 11053-11063, 10.1021/jp062836f, 2006.
868 Zhang, Q., Jimenez, J. L., Canagaratna, M. R., Ulbrich, I. M., Ng, N. L., Worsnop, D. R., and Sun, Y.
869 L.: Understanding atmospheric organic aerosols via factor analysis of aerosol mass spectrometry: a
870 review, Anal. Bioanal. Chem., 401, 3045-3067, 10.1007/s00216-011-5355-y, 2011.

871   Zhang, R. Y., Khalizov, A., Wang, L., Hu, M., and Xu, W.: Nucleation and Growth of Nanoparticles in
872   the Atmosphere, Chem. Rev., 112, 1957-2011, 10.1021/cr2001756, 2012.
873   Zhang, S. H., Shaw, M., Seinfeld, J. H., and Flagan, R. C.: Photochemical aerosol formation from
874   alpha-pinene- and beta-pinene, J. Geophys. Res.-Atmos., 97, 20717-20729, 1992.
875   Zhang, X., Cappa, C. D., Jathar, S. H., McVay, R. C., Ensberg, J. J., Kleeman, M. J., and Seinfeld, J.
876   H.: Influence of vapor wall loss in laboratory chambers on yields of secondary organic aerosol, Proc.
877   Nat. Acad. Sci. U.S.A., 111, 5802-5807, 10.1073/pnas.1404727111, 2014.
878   Zhang, X., Schwantes, R. H., McVay, R. C., Lignell, H., Coggon, M. M., Flagan, R. C., and Seinfeld, J.
879   H.: Vapor wall deposition in Teflon chambers, Atmos. Chem. Phys., 15, 4197-4214, 10.5194/acp-15-
880   4197-2015, 2015.
881   Zhao, D. F., Kaminski, M., Schlag, P., Fuchs, H., Acir, I. H., Bohn, B., Häseler, R., Kiendler-Scharr, A.,
882   Rohrer, F., Tillmann, R., Wang, M. J., Wegener, R., Wildt, J., Wahner, A., and Mentel, T. F.:
883   Secondary organic aerosol formation from hydroxyl radical oxidation and ozonolysis of monoterpenes,
884   Atmos. Chem. Phys., 15, 991-1012, 10.5194/acp-15-991-2015, 2015.
885   Zhao, D. F., Buchholz, A., Kortner, B., Schlag, P., Rubach, F., Fuchs, H., Kiendler-Scharr, A.,
886   Tillmann, R., Wahner, A., Watne, Å. K., Hallquist, M., Flores, J. M., Rudich, Y., Kristensen, K.,
887   Hansen, A. M. K., Glasius, M., Kourtchev, I., Kalberer, M., and Mentel, T. F.: Cloud condensation
888   nuclei activity, droplet growth kinetics, and hygroscopicity of biogenic and anthropogenic secondary
889   organic aerosol (SOA), Atmos. Chem. Phys., 16, 1105-1121, 10.5194/acp-16-1105-2016, 2016.
890   Ziemann, P. J., and Atkinson, R.: Kinetics, products, and mechanisms of secondary organic aerosol
891   formation, Chem. Soc. Rev., 41, 6582-6605, 10.1039/c2cs35122f, 2012.
892
893

Table 1 Overview of the experiments in this study

Precursor	SO$_2$	NO$_x$	NO (ppb)	SO$_2$ (ppb)
α-pinene	Low SO$_2$	Low NO$_x$	0.05-0.2	<0.05
		High NO$_x$	~20	<0.05
(~20 ppb)	High SO$_2$	Low NO$_x$	0.05-0.2	~15
		High NO$_x$	~20	~15
Limonene	Low SO$_2$	Low NO$_x$	0.05-0.2	<0.05
		High NO$_x$	~20	<0.05
(~7 ppb)	High SO$_2$	Low NO$_x$	0.05-0.2	~15
		High NO$_x$	~20	~15
	Moderate SO$_2$	High NO$_x$	~20	~2

896

897   (a)   (b)
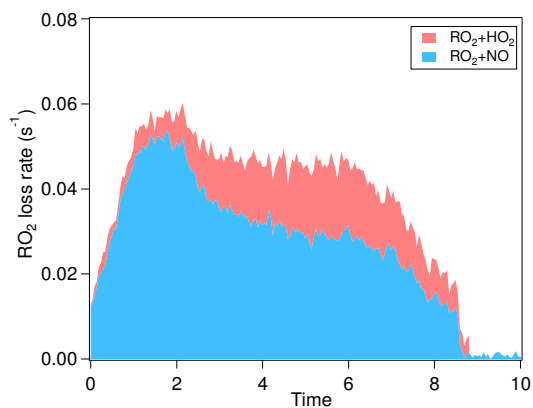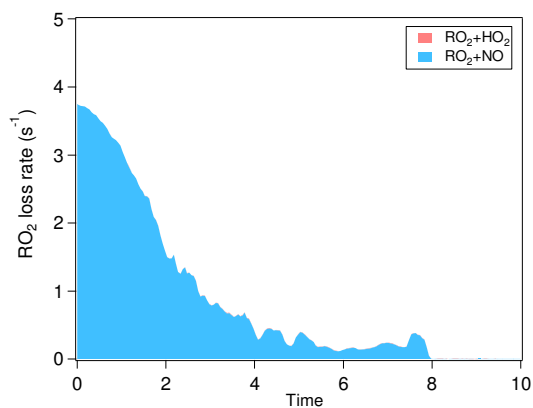
898   Figure 1. Typical loss rate of RO_2 by RO_2+NO and RO_2+HO_2 in the low NO_x (a) and the high NO_x (b) conditions

899   of this study. The experiments at low SO_2 are shown. The RO_2+HO_2 rate is stacked on the RO_2+NO rate. Note

900   the different scales for RO_2 loss rate in panel a and b. In panel b, the contribution of RO_2+HO_2 is very low and

901   barely noticeable.
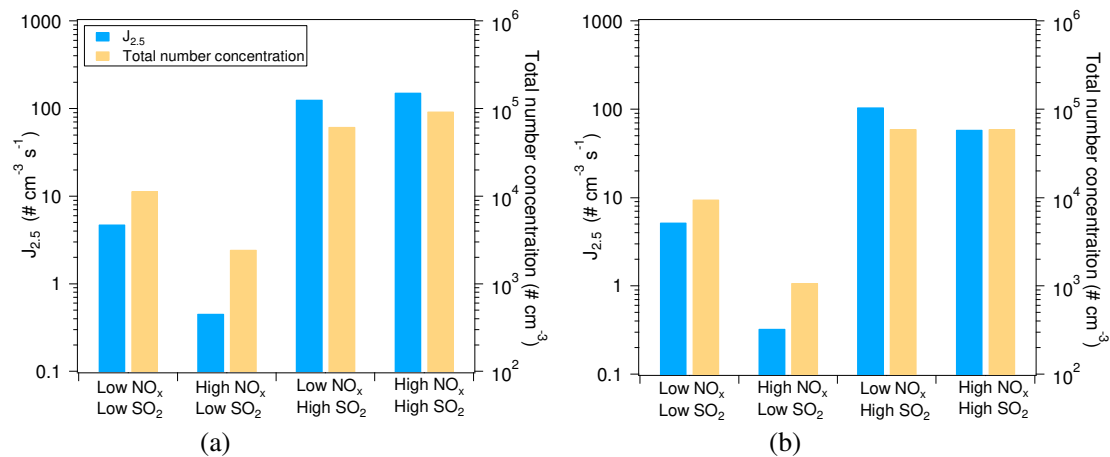
902
903 (a) (b)
904 Figure 2. Nucleation rates ($J_{2.5}$) and maximum total particle number concentrations under different NO_x and SO_2
905 conditions for the SOA from α-pinene oxidation (a) and from limonene oxidation (b).

906

907

(a)

908
909
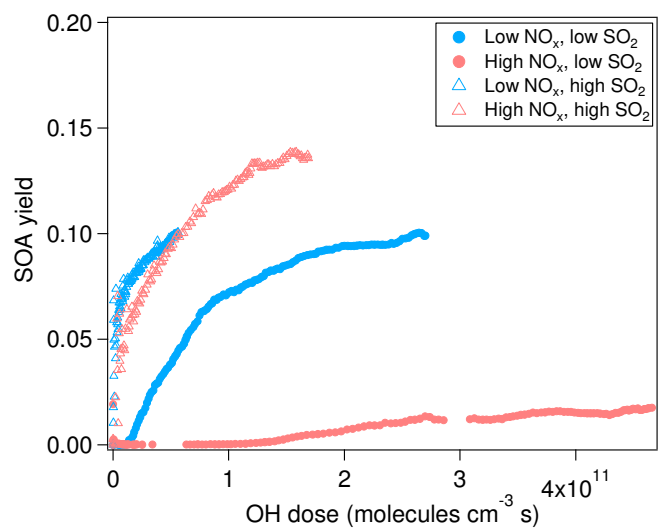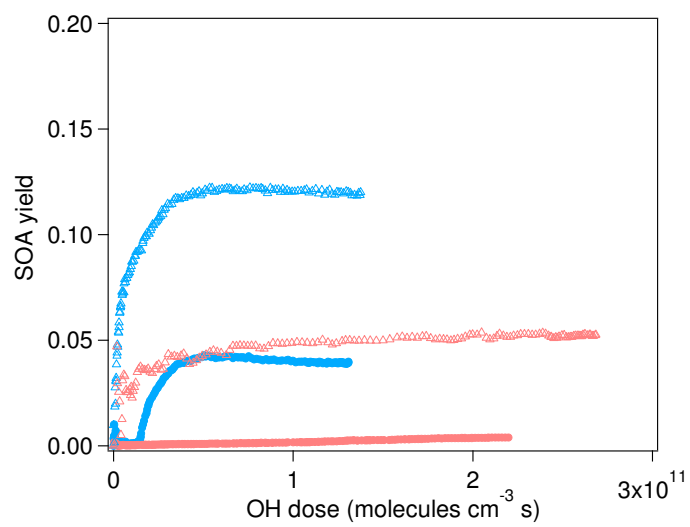
910
911   (b)
912   Figure 3. SOA yield of the photooxidation of α-pinene (a) and limonene (b) in different NO_x and SO_2 conditions.

913

914
915
(a)   (b)
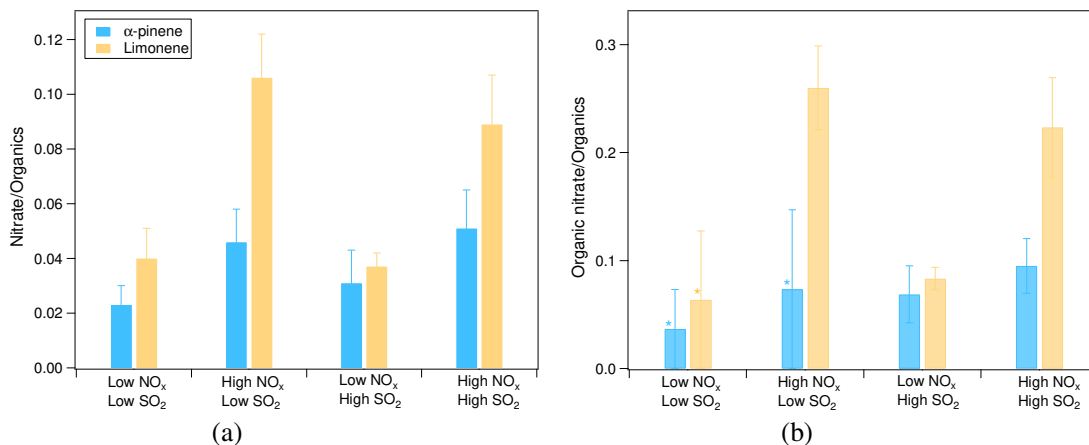
916 Figure 4. (a) The ratio of nitrate mass concentration to organics mass in different NO_x and SO_2 conditions. The

917 average ratios of nitrate to organics during the reaction are shown and error bars indicate the standard deviations.

918 (b) The fraction of organic nitrate to total organics in different NO_x and SO_2 conditions calculated using a

919 molecular weight of 200 g/mol for organic nitrate. The average fractions during the reaction are shown and error

920 bars indicate the standard deviations. In panel b, * indicate the experiments where the ratios of NO_2^+ to NO^+ were

921 too noisy to derive a reliable fraction of organic nitrate. For these experiments, 50% of total nitrate was assumed

922 to be organic nitrate and the error bars show the range when 0 to 100% of nitrate are assumed to be organic

923 nitrate.

925
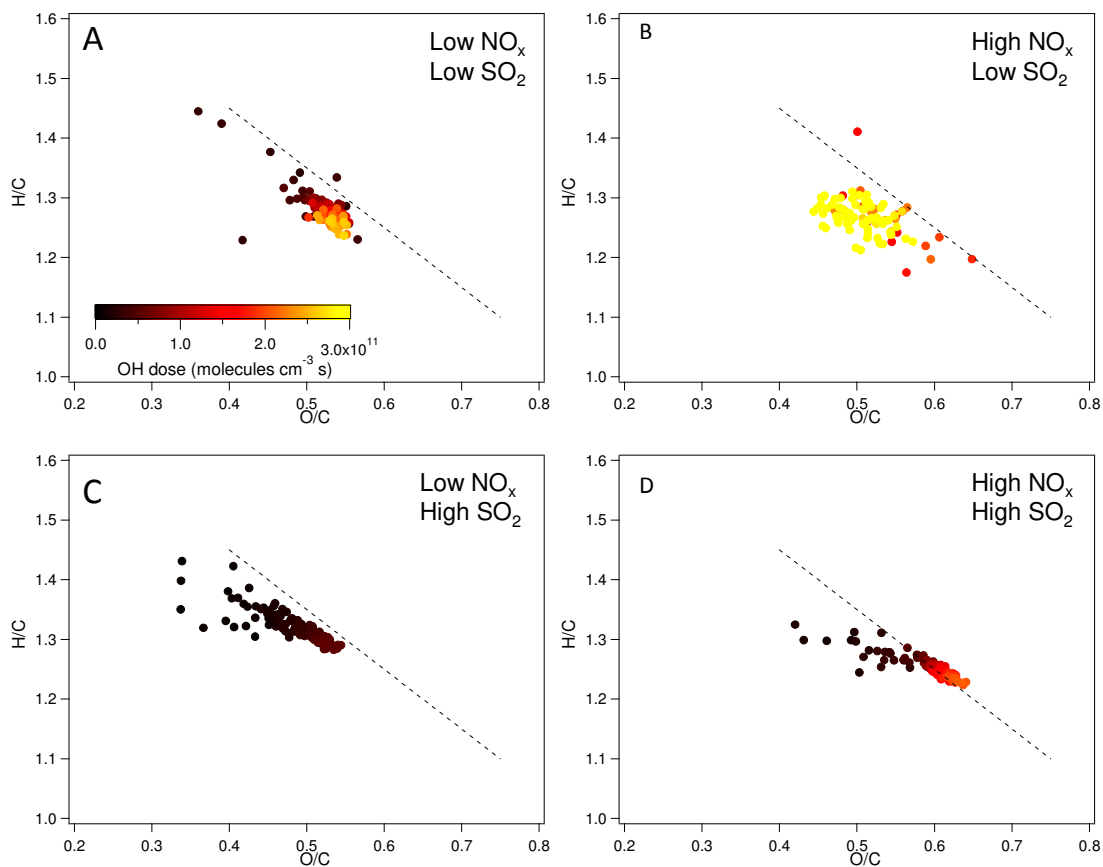
Figure 5. H/C and O/C ratio of SOA from photooxidation of α-pinene in different NO_x and SO_2 conditions. A: low NO_x, low SO_2, B: high NO_x, low SO_2, C: low NO_x, high SO_2, D: high NO_x, high SO_2. The black dashed line corresponds to the slope of -1.
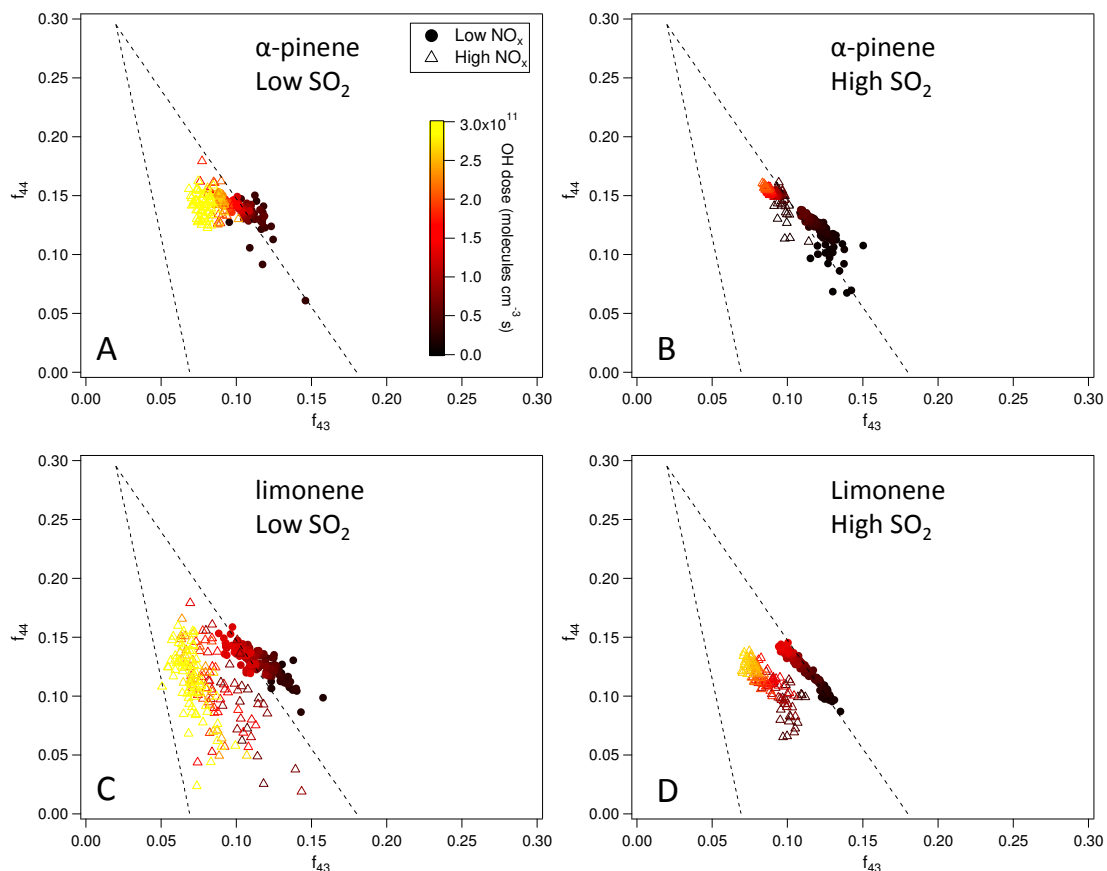
Figure 6. f_{44} and f_{43} of SOA from the photooxidation of α-pinene and limonene in different NO_x and SO_2 conditions. A: α-pinene, low SO_2, B: α-pinene, high SO_2, C: limonene, low SO_2, D: limonene, high SO_2. Note that in the low SO_2, high NO_x condition (panel C), the AMS signal of SOA from limonene oxidation was too low to derive reliable information due to the low particle mass concentration and small particle size. Therefore, the data for high NO_x in panel C show an experiment with moderate SO_2 (2 ppb) and high NO_x instead.
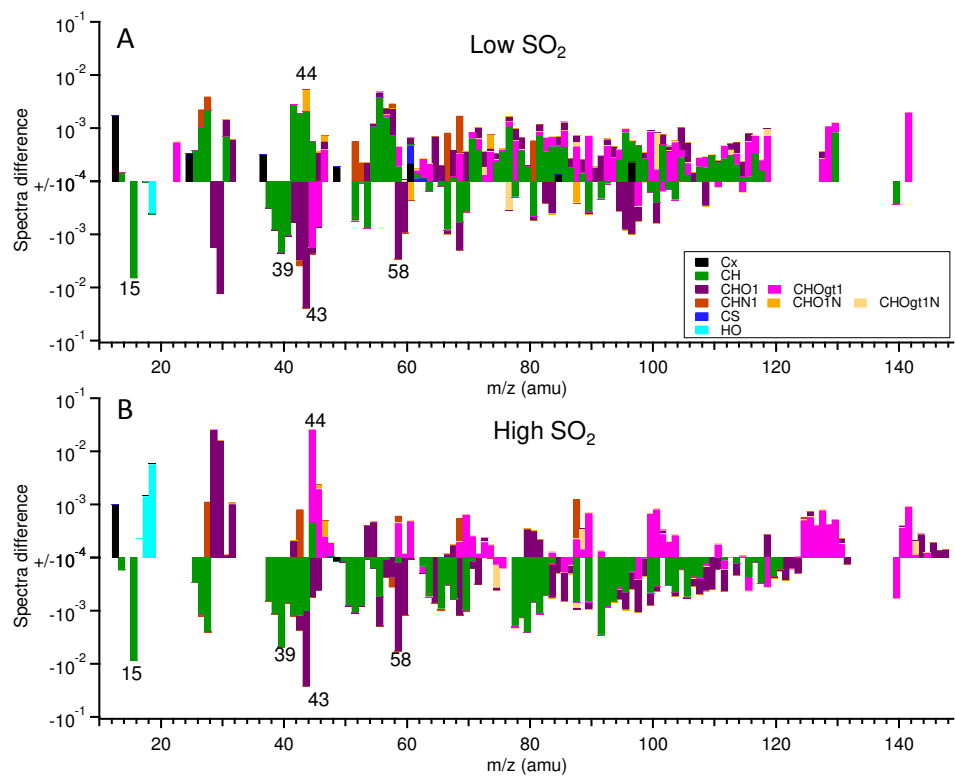
Figure 7. The difference in the mass spectra of organics of SOA from α-pinene photooxidation between high NO_x and low NO_x conditions (high NO_x-low NO_x). SOA was formed at low SO_2 (a) and high SO_2 (b). The different chemical family of high resolution mass peaks are stacked at each unit mass *m/z* ("gt1" means greater than 1). The mass spectra were normalized to the total organic signals. Note the log scale of y-axis and only the data with absolute values large than 10^{-4} are shown.

941
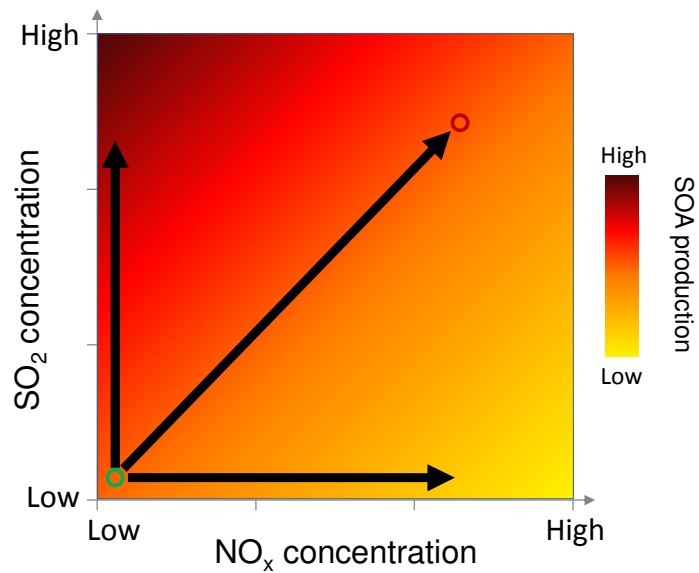
Figure 8. Conceptual schematic showing how NO_x and SO_2 concentrations affect biogenic SOA mass production. The darker colors indicate higher SOA production. The circle on the bottom left corner indicates biogenic cases and the circle on the right top corner indicates the anthropogenic cases. And the horizontal and vertical arrows indicate the effect of NO_x and SO_2 alone. The overall effects on SOA production depend on specific NO_x, SO_2 concentrations and VOC concentrations and speciation.